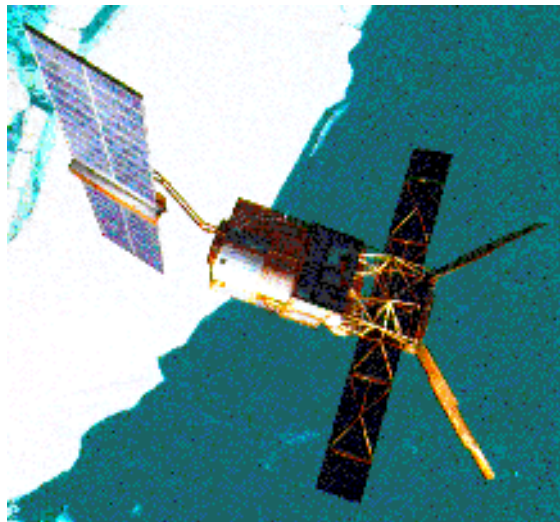


---

# ERS-2 Wind Scatterometer Cyclic Report

from 23<sup>rd</sup> April 2001 to 2<sup>nd</sup> July 2001  
Cycle 63 and Cycle 64



---

Prepared by:

PCS team

ESRIN EEM-ADQ

Inputs from:

F. Aidt  
H. Hersbach

ESTEC TOS-EMS  
ECMWF

Issue: 1.0  
Reference: ERSE-SPPA-EOAD-TN-01-0001  
Date of issue: 24<sup>th</sup> July 2001  
Status: Approved  
Document type: Technical Note  
Approved by: P. Lecomte



*P. Lecomte*

# Distribution List

(Summary only via e-mail)

|  |  |   |
|--|--|---|
| ESTEC  | M. Canela<br>E. Attema<br>M. Drinkwater<br>F. Aidt<br>B. Gelsthorpe<br>R. Zobl<br>K. van't Klooster  | EEM-LR<br>EEM-FSS<br>EEM-FSO<br>TOS-EMS<br>EEM-PTR                    |
| ESOC   | F. Bosquillon de Frescheville<br>L. Stefanov   | TOS-OFC<br>TOS-OFC  |
| ESRIN  | M. Albani<br>P. Lecomte<br>V. Beruti<br>S. Jutz<br>G. Kohlhammer<br>M. Onnestam<br>U. Gebelein   | EEM-AD<br>EEM-ADQ<br>EEM-ADF<br>EEM-ADU<br>EEM-AM<br>EEM-ADC<br>Serco |
| L.A. Breivik<br>P. Snoeij<br>J. Heidbreder<br>L. Isaksen, H. Hersbach<br>J. Kerkman, J. Figa<br>S. Pouliquen<br>V. Wismann<br>A. Cavanie<br>R.S. Dunbar<br>A. Stoffelen, T. Driessenaar<br>G. Legg, P. Chang<br>W. Gemmill<br>J. Hawkins<br>D. Offiler, R. Graham, C.A. Parrette<br>F. Courtier, H. Roquet<br>C. Scupniewicz<br>R.A. Brown<br>J. Boutin<br>M.A. Messeh | DNMI<br>DUT<br>DORNIER<br>ECMWF<br>EUMETSAT<br>F-PAF<br>IFARS<br>IFREMER<br>JPL<br>KNMI<br>NOAA/NESDIS<br>NOAA/NWS<br>NRL<br>UK-MET Office<br>Meteo-France<br>FNMOC<br>University of Washington<br>LODYC/UPMC<br>University of Sheffield |   |

This report and its annex (ECMWF report) are available on PCS web:  
<http://pcswww.esrin.esa.it>

## **1.0 Introduction and summary**

The document includes a summary of the daily quality control made within the PCS and various sections describing the results of the investigations and studies of “open-problems” related to the Scatterometer. In each section results are shown from the beginning of the mission in order to see the evolution and to outline possible “seasonal” effects. An explanation for the major events which have impacted the performance since launch is given, and comments about the recent events which occurred during the last cycle are included.

This report covers the period from 23<sup>rd</sup> April 2001 to 2<sup>nd</sup> July 2001 (cycle 63 and cycle 64).

### Mission events

- During the cycle 63 the ERS-2 satellite was in EBM-YSM.
- From 22<sup>nd</sup> May to 24<sup>th</sup> May 2001 the satellite payload was switched-off due to platform anomaly and on 25<sup>th</sup> May the AMI instrument was switched-off due to thermal analysis. This last event was monitored by PCS and ESOC. The increase of temperatures was due to the Payload Heaters which were left on even if the instrument was in operative mode. The impact on the Scatterometer was a lower transmission power. The problem was solved on 25<sup>th</sup> May and the temperatures as well as the transmitted power returned to the nominal level.
- On 6<sup>th</sup> June 2001 a AOCS software patch called Zero Gyro Mode (ZGM) was up-linked on the satellite. The ZGM was activated on 7<sup>th</sup> June 2001. Its scope is to improve the attitude performances along the yaw axis. The tuning of the new software by ASTRIUM-ESOC-ESRIN continued for large part of cycle 64 as the satellite was in ZGM commissioning phase.
- During the ZGM commissioning phase the AMI instrument was operated in wind-wave mode throughout the whole orbit. This mode allow to estimate yaw error angle along the orbit by analysing the SAR imagette.
- During the cycle 63 and cycle 64 no Scatterometer products were disseminated to the users due to poor quality of the sigma nought retrieved by the current algorithm.
- For that reason the Ocean calibration monitoring and the winds monitoring performed by ECMWF was not carried out.
- The PCS continues its mission monitoring and results are given in the following paragraphs.

### Calibration performance

- Due to EBM operations and ZGM commissioning phase the Scatterometer sigma noughts are not calibrated until a new version of the ground processor is implemented.
- The sigma noughts (and as consequence the Gamma noughts) acquired over the Rain Forest show a very high fluctuation due to degraded satellite attitude.
- The dynamic of the Gamma nought ranges from -15 dB to -5 dB (the nominal range was -6 dB, -7dB) and the corresponding histograms are very noisy with a high standard deviation.
- The Transponders were working nominally during the calibration passes but the CALPROC system is not able to process any more the data acquired in EBM: the results are meaningless. For that reason new gain constant will not available until a new version of CALPROC is implemented.

### Instrument performance

- During the cycle 63 and cycle 64 the power decrease was on average 0.18 dB/cycle. This result does not confirm the zero trend reported in the previous report. The actual level of the transmitted power is roughly 0.36 dB below the level reached in October 1998 and therefore a new power increase shall be agreed with ESOC.
- The monitoring of the Doppler frequency shows a regular improvement during the ZGM commissioning phase. In particular the daily average standard deviation of the CoG of the received spectrum decreased from 7000 Hz to 5200 Hz for the Fore and Aft antenna and from 6300 Hz to 5700 Hz for the Mid antenna. This fact indicates an improvement in the yaw performances as confirmed by the wave data.
- During cycle 63 the monitoring of the noise power shows a stable result.
- During the cycle 64 the monitoring of the noise shows a decrease of the noise power starting from 6<sup>th</sup> June 2001. This noise power decrease could be linked with the beginning of wind-wave operation throughout the whole orbit.
- The monitoring of the antennae temperature over the Brazilian Rain Forest shows a stable result for the ascending passes. At the descending passes the seasonal increase of the antenna temperatures has a different behaviour for the Fore and Aft antenna. In particular during the cycle 64 the Fore antenna temperature had an increase of roughly 3 degrees. This could be related with the instability in the satellite attitude (change of the incidence angle between the antenna panel and the Sun light at the descending passes).

### Product performance

- During the cycle 63 the quality of the products was very poor and no improvements has been seen. The wind speed bias (ECMWF forecast Vs UWI) was around 1.5 m/s.
- During the cycle 64 in relation to ZGM commissioning phase a small improvement has been seen in the UWI products. In particular the number of valid nodes progressively passed from 9000 per day to 16000 per day. The reason was an increase of the signal to noise ratio related to the improvements of the yaw performances during the ZGM campaign. No improvements were seen in the wind speed bias (ECMWF forecast Vs UWI) and in the related standard deviation.

## 2.0 Calibration Performances

The calibration performances are estimated using three types of target: a man made target (the transponder) and two natural targets (the rain forest and the ocean). This approach allow us to design the correct calibration using a punctual but accurate information from transponders and an extended but noisy information from rain forest and ocean for which the main component of the variance comes from the geophysical evolution of the natural target and from the backscattering models used. These aspects are in the calibration performance monitoring philosophy. The major goals of the calibration monitoring activities are the achievement of a “flat” antenna pattern profile and the assurance of a stable absolute calibration level.

### 2.1 Gain Constant over transponder

One gain constant is computed per transponder per beam from the actual and simulated two-dimensional echo power, which is given as a function of the orbit time and range time. This parameter clearly indicates the difference between “real instrument” and the mathematic model. In order to acquire data over the transponder the Scatterometer must be set in an appropriate operational mode defined as “Calibration Mode”.

Table 1 shows the result of the calibration plan for cycle 63 and 64. The “Yes” in the EWIC column means that the raw data are available, “No” means that some problems caused a loss of data. The “On” in the transponder status column means that, from the raw data (EWIC), the transponders have been recognised as switched-on; “Off” that they were off. The “Yes” in the GC computed column means that a gain constant value has been retrieved, “No” means the opposite case. As reported in Table 1 the calibration plan, during the cycle 63 and cycle 64 was executed as planned but due to the degraded attitude the calibration data are meaningless. For that reason no new gain constant will be available until a new version of CALPROC is implemented. Furthermore it is not even possible, from the received data, to recognise if the transponder was switched on or not.

**TABLE 1. Calibration Plan: Cycle 63 and Cycle 64**

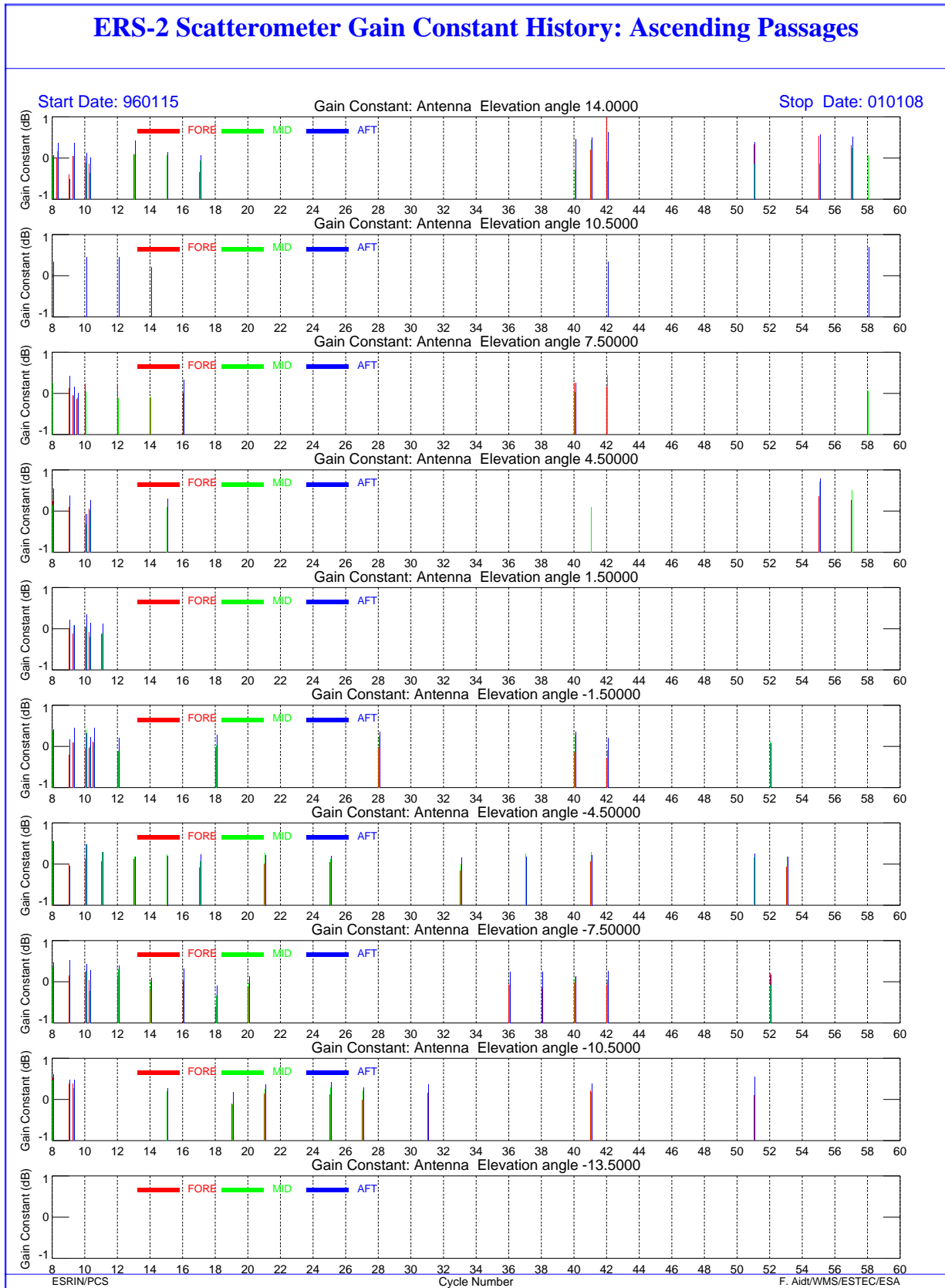
| DATE   | ORBIT<br>(absolute) | ORBIT<br>(relative) | Passage | Ground<br>Station | EWIC<br>(raw data) | AMI mode    | Transponder<br>Status | GC<br>computed |
|--------|---------------------|---------------------|---------|-------------------|--------------------|-------------|-----------------------|----------------|
| 010424 | 31425               | 8                   | D       | KS                | Yes                | Calibration | n/a                   | n/a            |
| 010427 | 31468               | 51                  | D       | KS                | Yes                | Calibration | n/a                   | n/a            |
| 010512 | 31690               | 273                 | A       | MS                | Yes                | Calibration | n/a                   | n/a            |
| 010515 | 31733               | 316                 | A       | MS                | Yes                | Calibration | n/a                   | n/a            |
| 010528 | 31919               | 1                   | A       | KS                | Yes                | Calibration | n/a                   | n/a            |
| 010531 | 31962               | 44                  | A       | MS                | Yes                | Calibration | n/a                   | n/a            |
| 010614 | 32155               | 237                 | D       | KS                | Yes                | Calibration | n/a                   | n/a            |
| 010617 | 32198               | 280                 | D       | KS                | Yes                | Calibration | n/a                   | n/a            |

Figure 1 and Figure 2 show the valid gain constants available **since the beginning of the mission until cycle 60 (end of mono-gyro operation)**. The analysis is made for various antenna elevation

angle. From these figures it is clear that the gain constant measurements are stable (within +/-0.5 dB).

The plots in Figure 3 show the value of the Gain Constant for the three beams and for the ascending, descending and all passes. The plots show the average of all gain constants available since January 1996 (cycle 8) for each antenna elevation angle. The antenna patterns are flat but there is a clear shift of the level of the curves. On average, the mid beam is 0.3 dB higher than the aft one and 0.5 dB higher than the fore one. For the descending passes the antenna pattern shows a slight negative slope from far range to near range.

Since September 1996, ESTEC has added a scaling factor to the gain constant in order to remove the bias among the three antennae. The gain constants were increased by 0.2 dB, -0.3 dB and 0.2 dB, for the fore, mid and aft beam respectively. The result is shown in Figure 4. The suggestion given by ESTEC has not been introduced into the ground processing because the antenna patterns computed over the rain forest do not show such bias (see Figure 5). So in the actual scenario, the differences among the antennae are considered as a bias due to the transponder themselves.



**FIGURE 1. ERS-2 Scatterometer; gain Constant over transponder since the beginning of the mission until cycle 60 (ascending passes).**

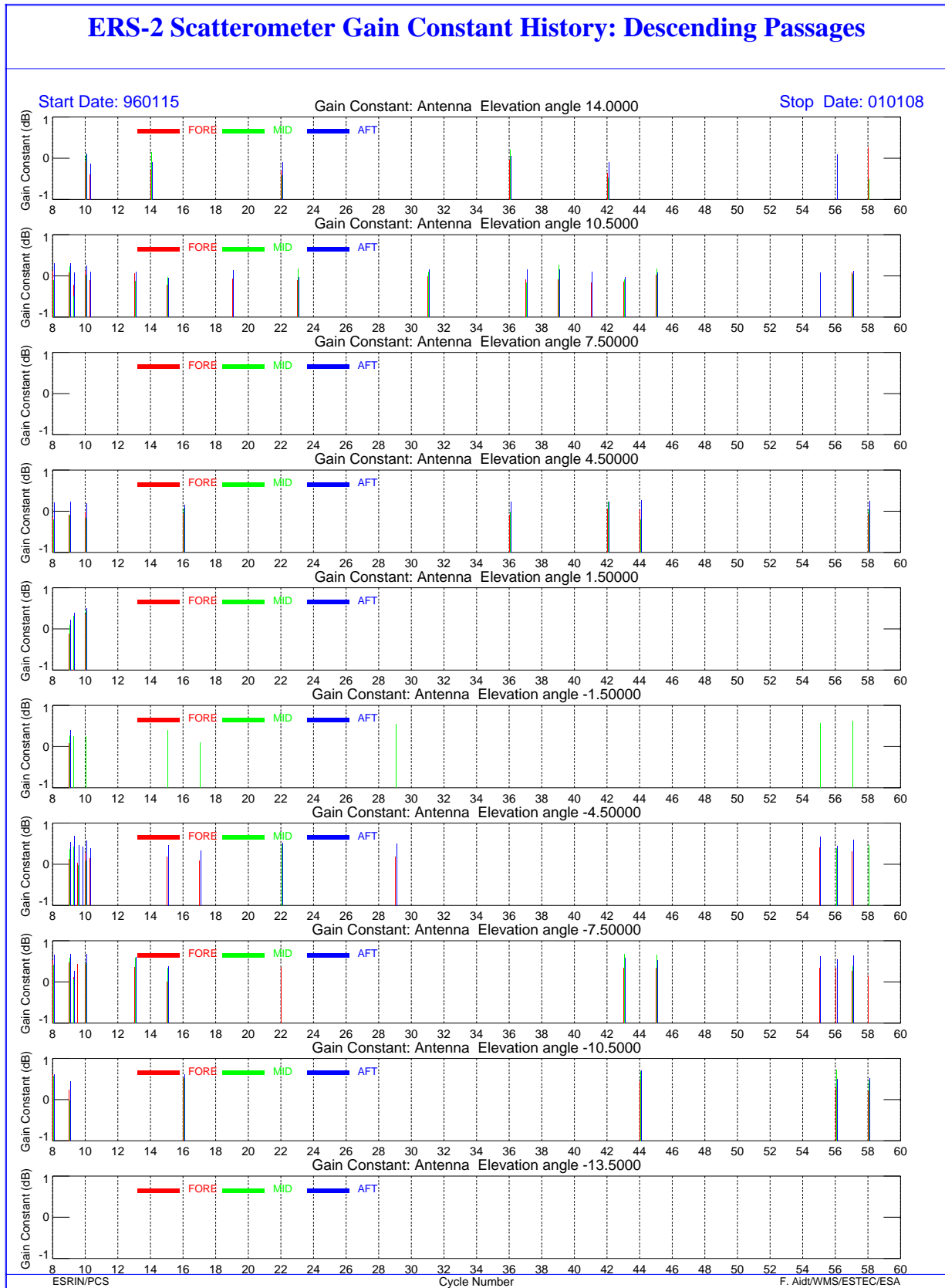


**FIGURE 2.** Scattermeter; gain Constant over transponder since the beginning of the mission until cycle 60 (descending passes)

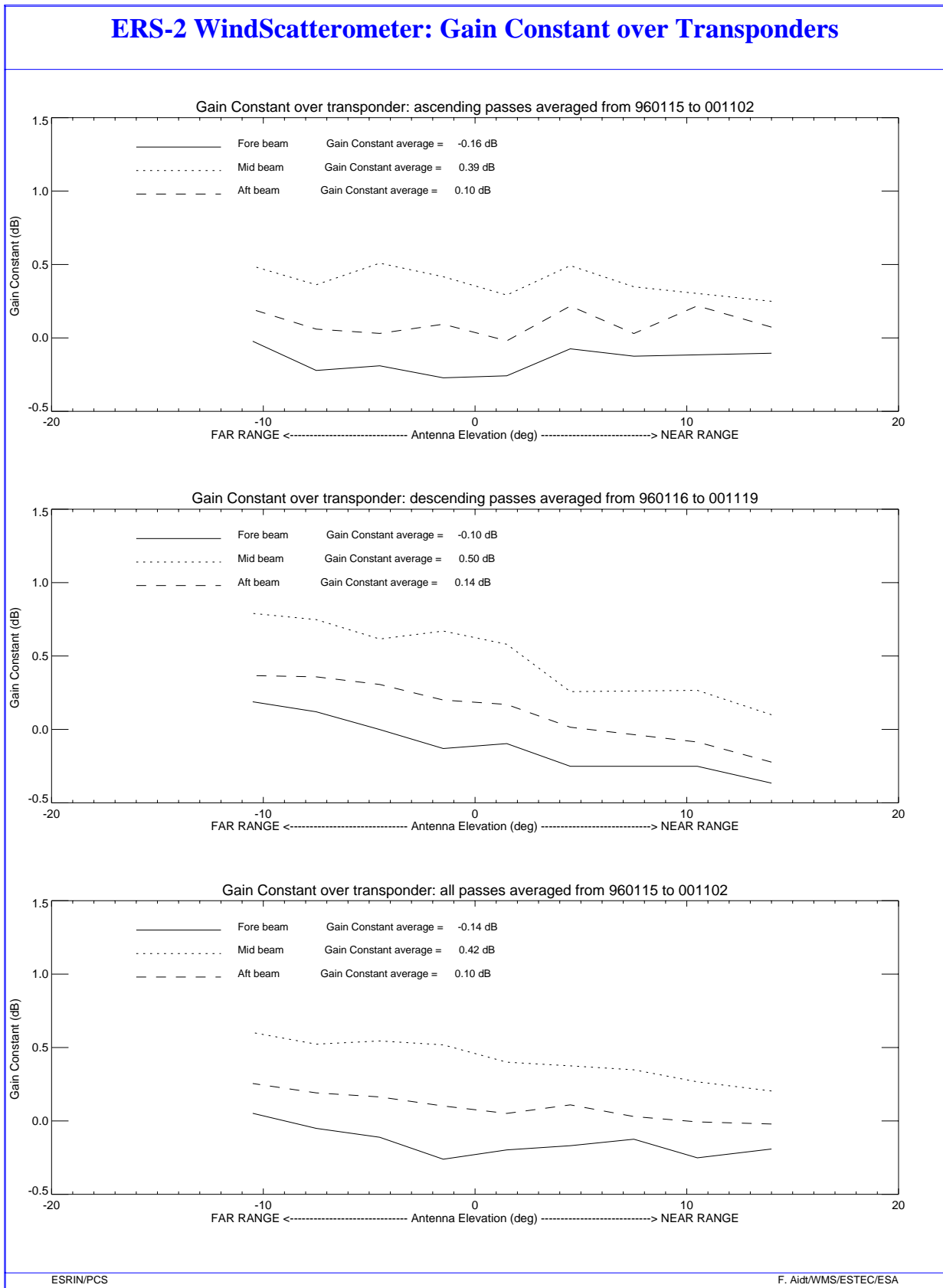


**FIGURE 3. ERS-2 Scatterometer: gain constant over transponders. All data available since January 1996 until cycle 60. Upper plot: ascending passes. Middle plot: descending passes. Lower plot: all passes.**

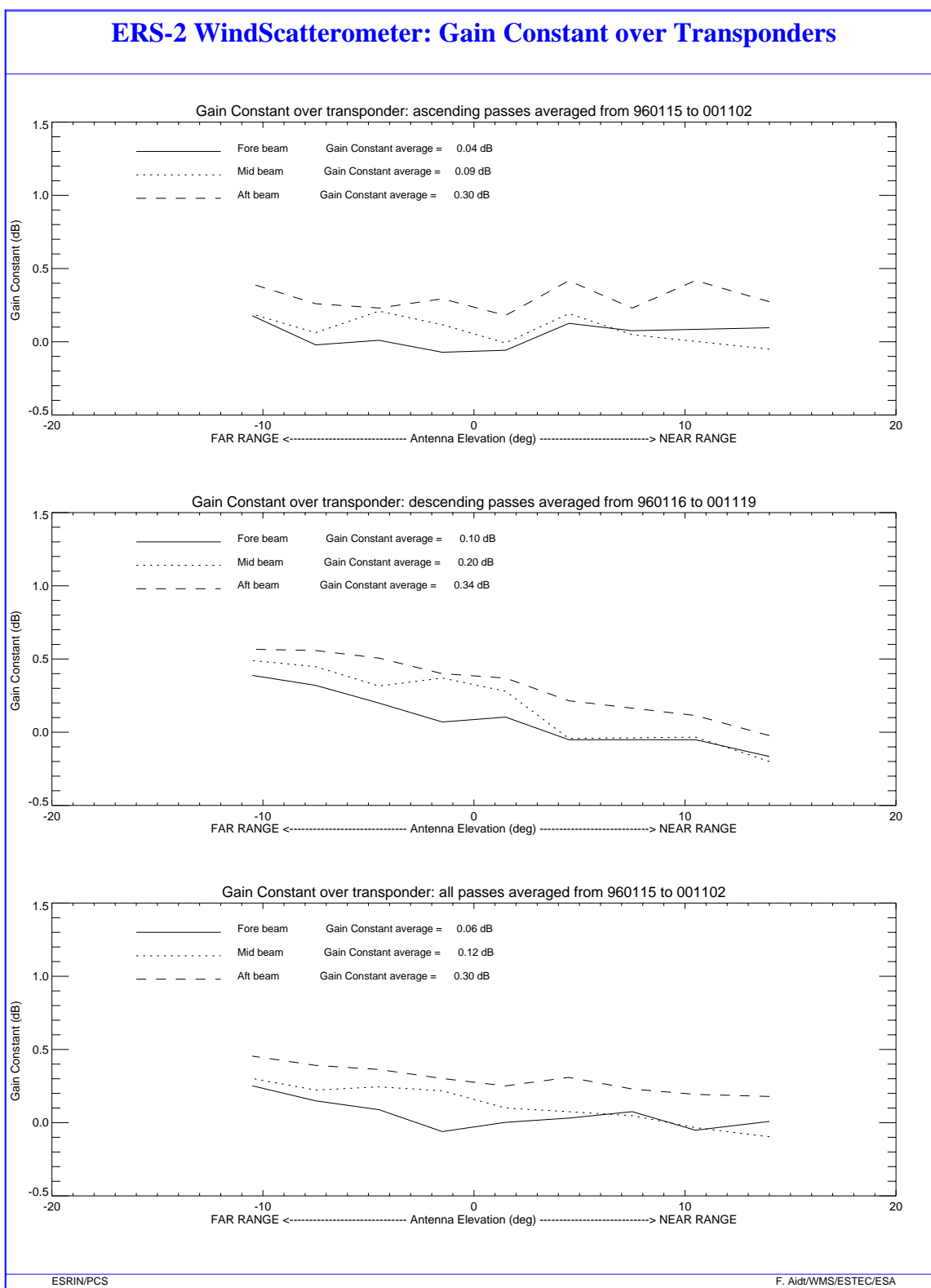


**FIGURE 4. ERS-2 Scatterometer: gain constant over transponders plus a scaling factor. All data available since January 1996 until cycle 60). Upper plot: ascending passes. Middle plot: descending passes. Lower plot: all passes.**

## 2.2 Ocean Calibration

During the cycle 63 and cycle 64 no Scatterometer data were disseminated to the users. For that reason the Ocean calibration monitoring performed by ECMWF was not carried out.

## 2.3 Gamma-nought over Brazilian rain forest

Although the transponders give accurate measurements of the antenna attenuation at particular points of the antenna pattern, they are not adequate for fine tuning across all incidence angles, as there are simply not enough samples. The tropical rain forest in South America has been used as a reference distributed target. The target at the working frequency (C-band) of ERS-2 Scatterometer acts as a very rough surface, and the transmitted signal is equally scattered in all directions (the target is assumed to follow the isotropic approximation). Consequently, for the angle of incidence used by ERS-2 Scatterometer, the normalised backscattering coefficient (sigma nought) will depend solely on the surface effectively seen by the instrument:

$$S^0 = S \cdot \cos \theta$$

With this hypothesis it is possible to define the following formula:

$$\gamma^0 = \frac{\sigma^0}{\cos \theta}$$

Using this relation, the gamma nought backscattering coefficient over the rain forest is independent of the incident angle, allowing the measurements from each of the three beams to be compared.

The test area used by the PCS is located between 2.5 degrees North and 5.0 degrees South in latitude and 60.5 degrees West and 70.0 degrees West in longitude.

The following paragraphs give a description of the activities carried out with this natural target.

### 2.3.1 Antenna pattern: Gamma-nought as a function of elevation angle

This analysis is normally carried out by ESTEC that has selected a larger region than the one used as test area by the PCS. In this case the selected rain forest extends from 2.0 degrees South to 11.0 degrees South in latitude and 56.0 degrees West to 80 degrees West in longitude. This large area was selected in order to increase the number of measurements.

For cycle 63 and cycle 64, the antenna patterns in function of the elevation angle have not been computed by ESTEC.

**2.3.2 Antenna pattern: Gamma-nought as a function of incidence angle**

Figure 5 and Figure 6 show the antenna patterns as a function of the incidence angle for cycle 63 and cycle 64 respectively.

The bad shape of the antennas pattern is due to operation in EBM and ZGM commissioning phase. The variations of the satellite attitude around the orbit explains the differences found among the antennas (the same area is viewed by the three antennas at different time).

**Note that the vertical scale of Figure 5 was changed to take into account the EBM data.**

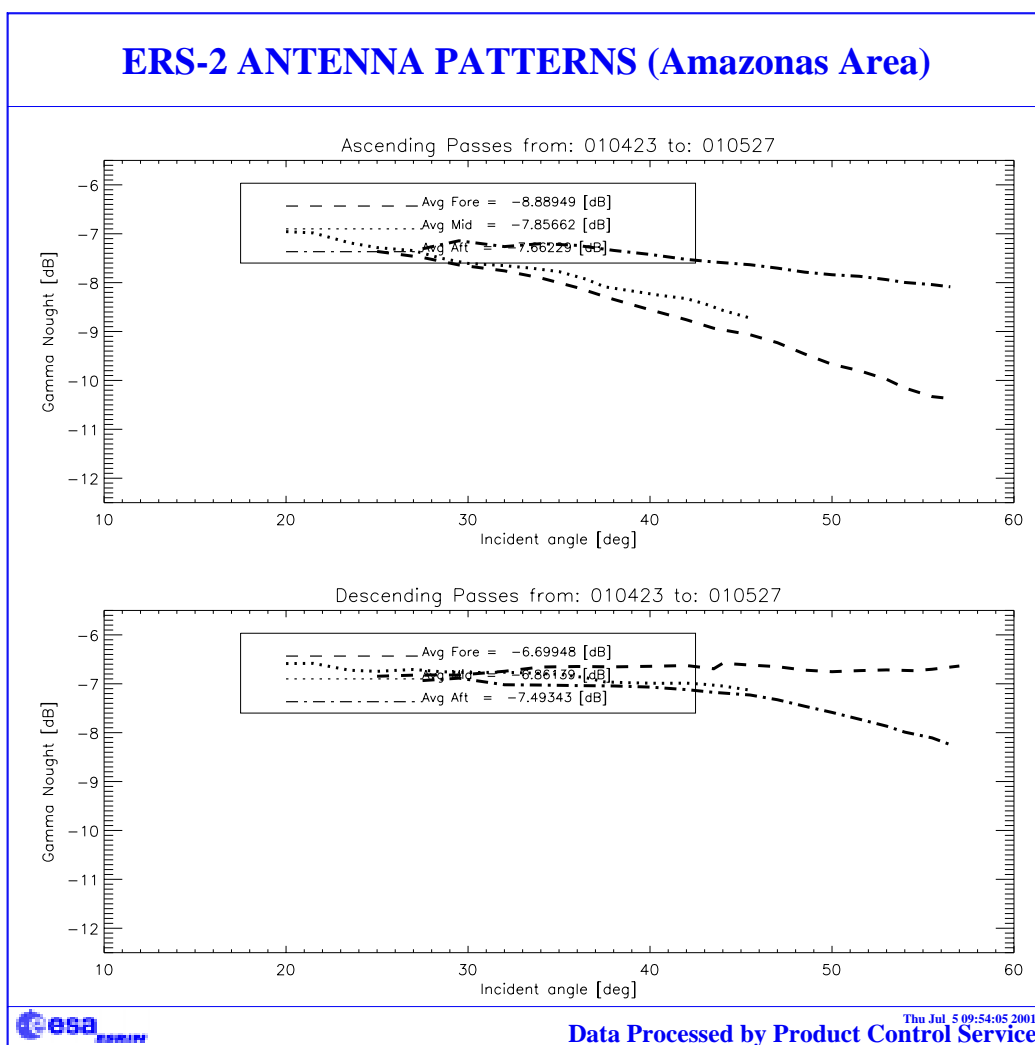


**FIGURE 5. ERS-2 Scatterometer antenna patterns as function of the incidence angle: cycle 63.**

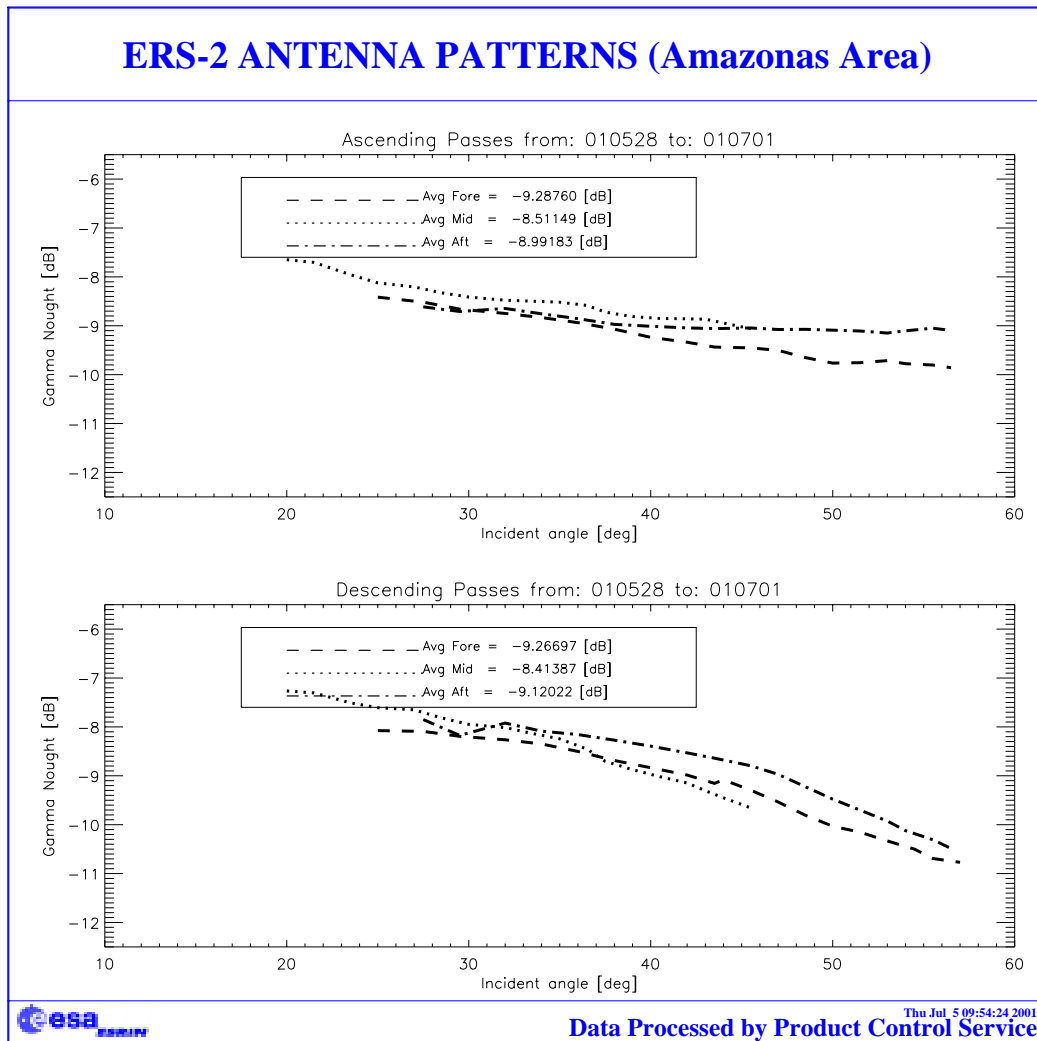


**FIGURE 6. ERS-2 Scatterometer antenna patterns as function of the incidence angle: cycle 64.**

### 2.3.3 Gamma nought histograms and peak position evolution

As the gamma nought is independent from the incidence angle, the histogram of gamma noughts over the rain forest is characterised by a sharp peak. The time-series of the peak position gives some information on the stability of the calibration. This parameter is computed by fitting the histogram with a normal distribution added to a second order polynomial:

$$F\langle x \rangle = A_0 \cdot \exp\left(-\frac{z^2}{2}\right) + A_3 + A_4 \cdot x + A_5 \cdot x^2$$

where: 
$$z = \frac{x - A_1}{A_2}$$

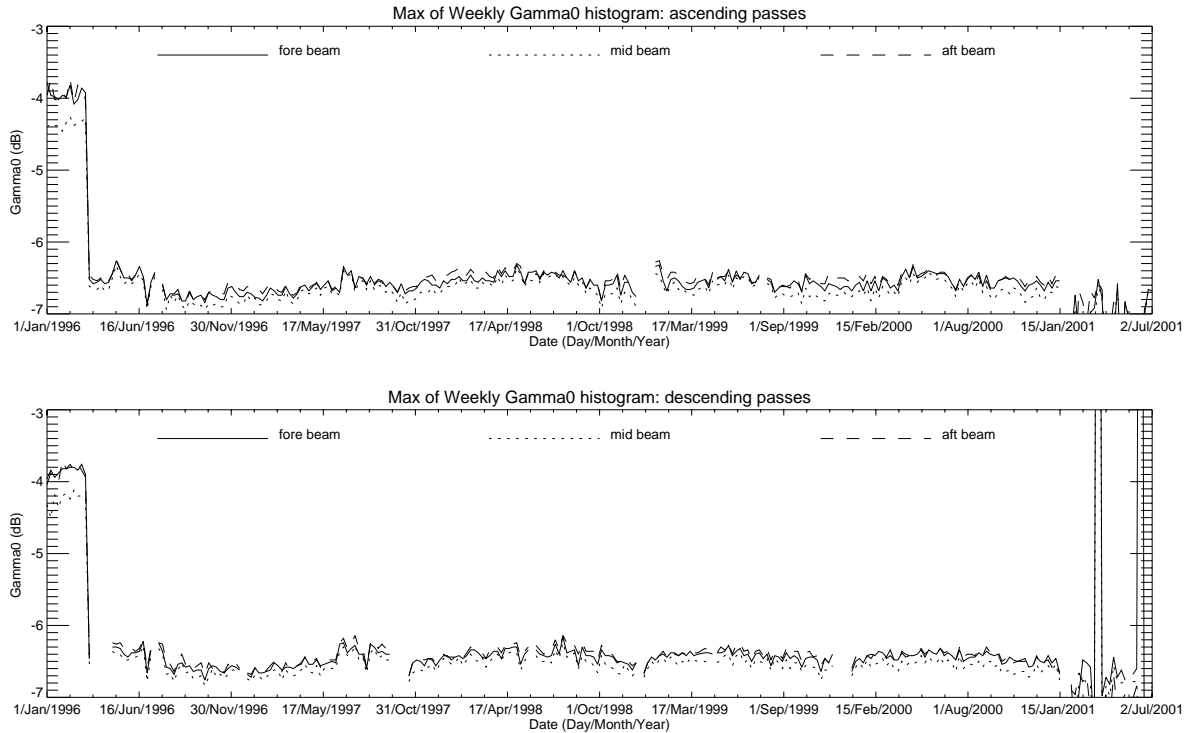
The parameters are computed using a non linear least square method called “gradient expansion”. The position of the peak is given by the maximum of the function  $F(x)$ . The histograms are computed weekly (from Monday to Sunday) for each antenna individually (“Fore”, “Mid”, and “Aft”) and for ascending and descending passes with a bin size of 0.02 dB.

Figure 6 shows the evolution of the histograms peak position since January 1996. The step shown in March 1996 is due to the end of commissioning phase when a new Look Up Table was used in the ground stations for WSCATT FD-products generation. It is interesting to note the decrease of roughly 0.2 dB from August 1996 to June 1997. This is linked to the switch of the Scatterometer calibration subsystem from side A to side B on 6<sup>th</sup> of August. The redundancy of side A device caused a little change in the calibration that was corrected on 19<sup>th</sup> June 1997 with a new calibration LUT used in the ground processing.

Figure 7 shows the evolution of the peak position corrected with the new calibration set also for the period from August 1996 to June 1997. The plots in Figure 7 show that the calibration stability achieved over the rain forest is within 0.5 dB. A seasonal effect is also present in the peak position evolution for the three antennae.

After the 17<sup>th</sup> January 2001 a meaning full monitoring of the peak position is not possible any more. Due to satellite degraded attitude the signal from Rain Forest is not stable, and the histograms’ shape (see figures from 11 to 20) does not show a sharp peak. This explains the high fluctuation in the time series from January 2001 onwards.

The actual AOCS configuration (called ZGM) gives a coarse attitude control in particular for the yaw angle. This causes a large Doppler shift (see also section 3.1) in the received echo that is not compensated for in the ground processing. The result is that Scatterometer products are not calibrated. A re-design of the Scatterometer data processor shall be performed to restore the initial data quality.



**FIGURE 7. ERS-2 Scatterometer, gamma-nought histogram: weekly evolution of maximum position. From up to down: ascending passes, descending passes.**

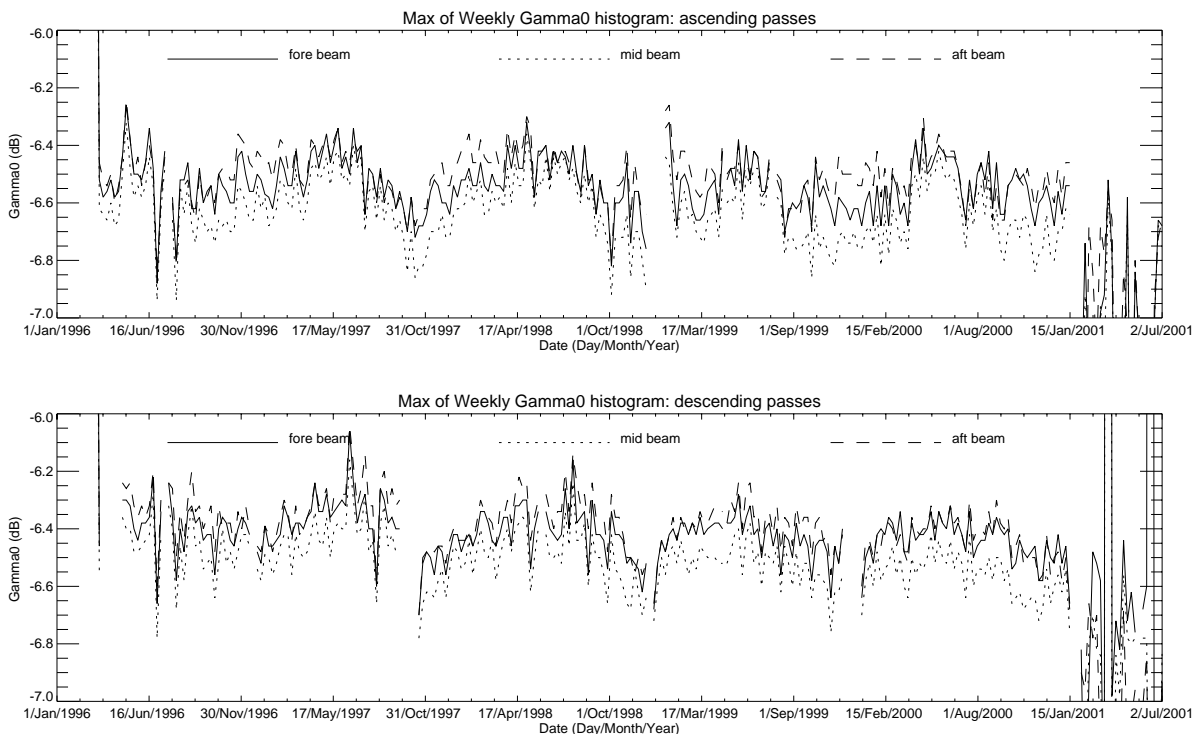


**FIGURE 8. Gamma-nought histogram: weekly evolution of maximum position. Data from 6<sup>th</sup> of August 1996 to 19<sup>th</sup> June 1997 are corrected with the new calibration constant (+0.2dB). Upper plot: ascending passes. Lower plot: descending passes.**

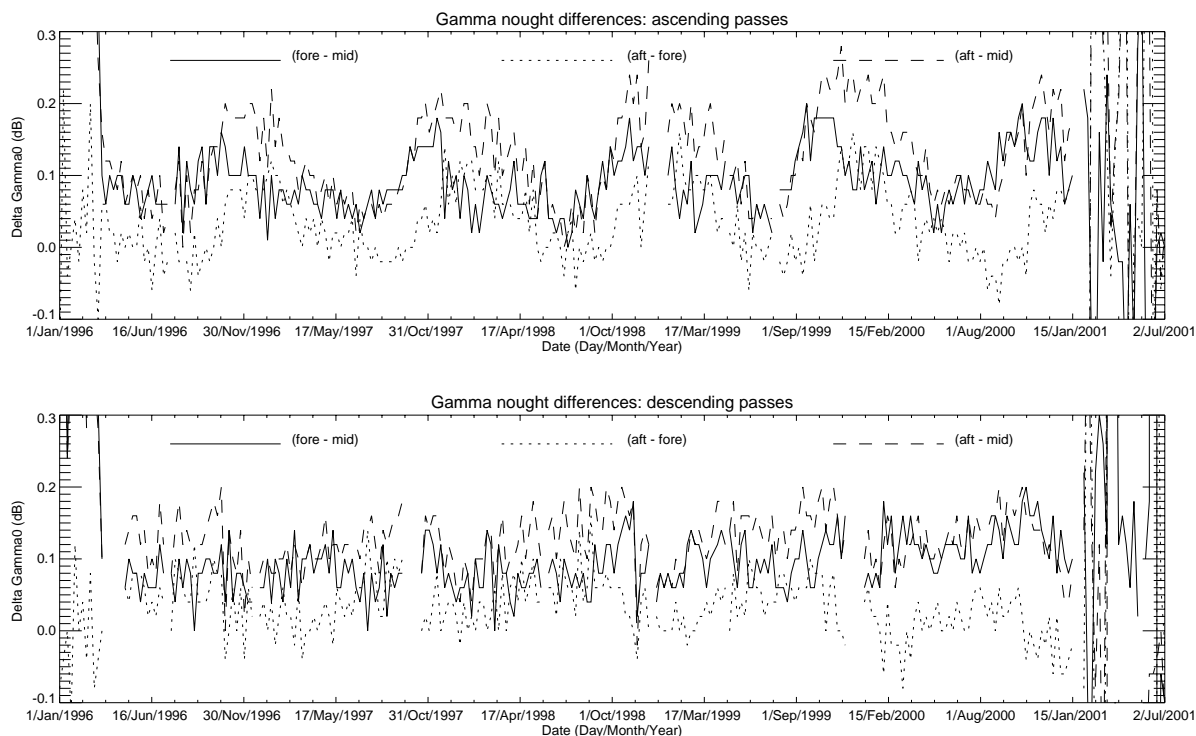


**FIGURE 9. Inter-beam calibration, weekly differences of the maximum position since 1<sup>st</sup> January 1996. From up to down: ascending passes, descending passes.**

For the inter-beam calibration, the results since 1996 are shown in Figure 9.

For the ascending passes, the differences in the signals have a seasonal behaviour. On average the differences are close to 0.1 dB during the summer and they are close to 0.2 dB during the winter. For the descending passes, the differences between the winter and the summer are less clear and the inter-beam calibration is around 0.1 dB (-0.03 dB for the aft-fore signal during the cycle 59).

A change around the end of year 1999 and the beginning of year 2000 is clearly present in the (aft-fore) difference signal as well as in the (aft-mid) signal. Investigations have been carried out in order to recognize which antenna has caused the change in the inter-beam calibration (see the report for the cycle 53). It can be noted that this evolution has mainly affected the Aft antenna with a mean decrease of roughly 0.05 dB in the signal. Because of the noise in the time series, it is also difficult to estimate if this evolution is related to mission or instrument events. The most relevant mission events were: the payload switch-off to face out the Leonid meteorite shower (November 1999), a series of AMI emergency switch down anomalies and the AOCS mono-gyro configuration (February 2000).

The mean and the standard deviation of the gamma-noughts are weekly computed directly using the Fast Delivery data. Figure 10 shows the evolution of the standard deviation since September 1996. The ascending passes show a gamma nought standard deviation higher than the descending ones. This can be explained because at ascending passes the test site appears less homogeneous; in particular for some areas near the rivers (see gamma nought images before cycle 60). The last plot in Figure 10 shows the number of valid measurements used to compute the statistics. A re-

duction of the number of valid observation since the beginning of 1999 can be seen. This is due to an increase of SAR images acquired over the Amazon rain forest.

The high values of the gamma nought standard deviations during the cycle 63 and cycle 64 are due to data acquired in EBM and during the ZGM commissioning phase (see section 3.1).

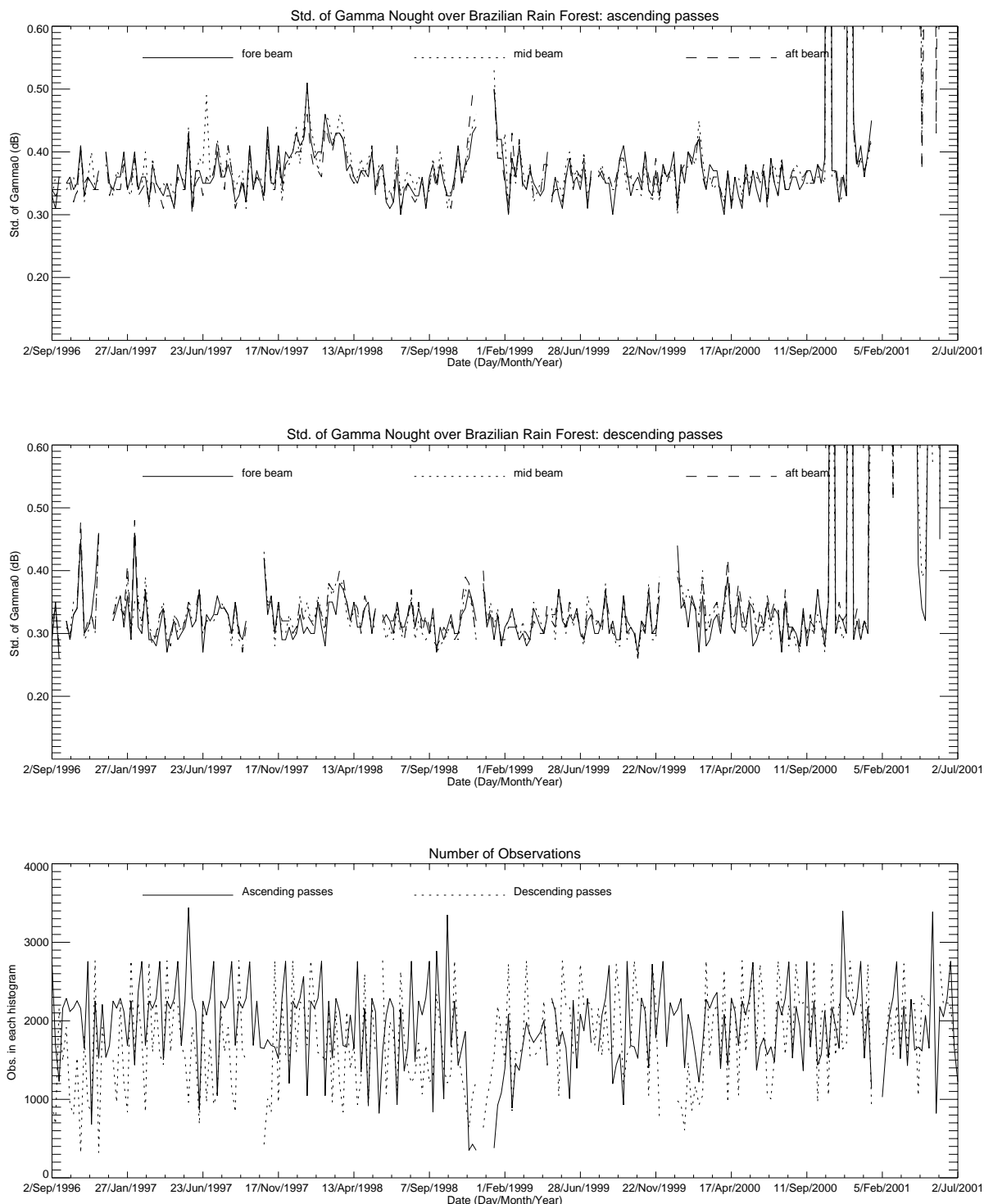


**FIGURE 10. Gamma-nought histograms: weekly evolution of standard deviation. From up to down: ascending passes standard deviation, descending passes standard deviation, number of valid observations.**

The Figures from 11 to 20 show the gamma nought histogram over the Brazilian rain forest throughout cycle 63 and cycle 64.

The histograms for the cycle 63 and cycle 64 show in general a very bad quality due to operations in EBM and ZGM commissioning phase. An improvement of the histogram's shape is seen for the ascending passes during the last two weeks of cycle 64.

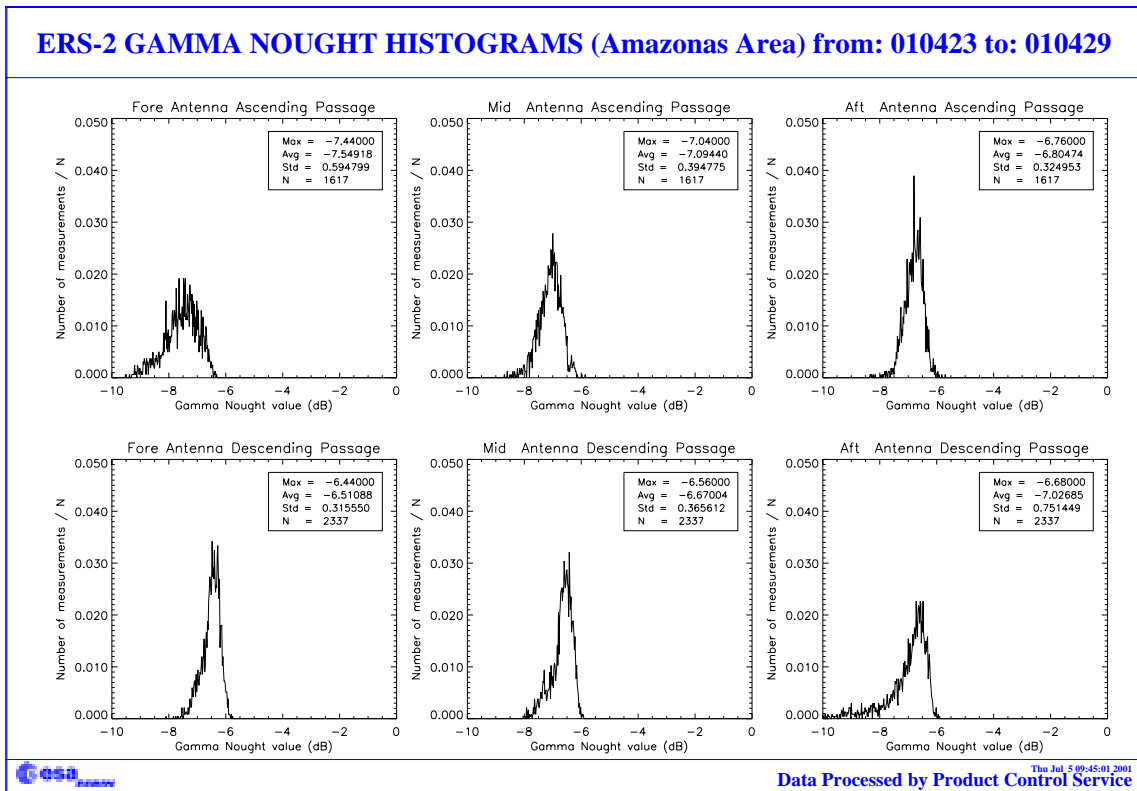


FIGURE 11. Gamma-nought histograms over Brazilian Rain forest: first week of the cycle 63.

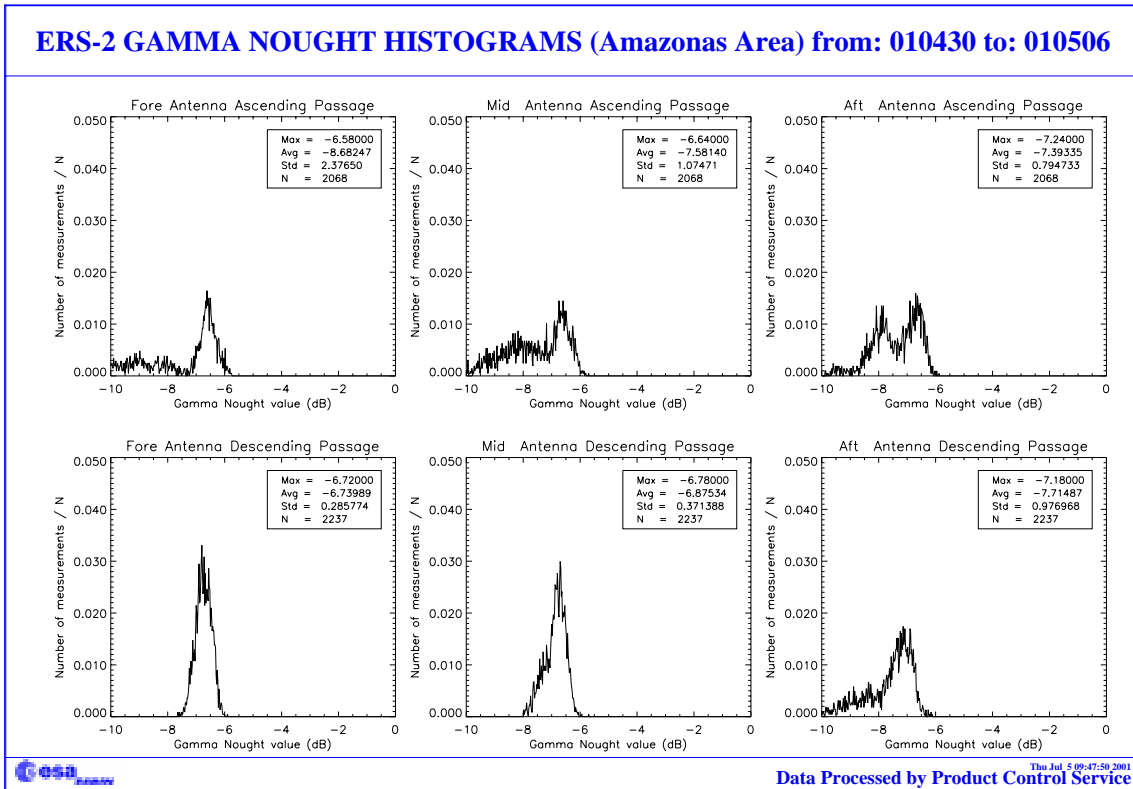


FIGURE 12. Gamma-nought histograms over Brazilian Rain forest: second week of the cycle 63.

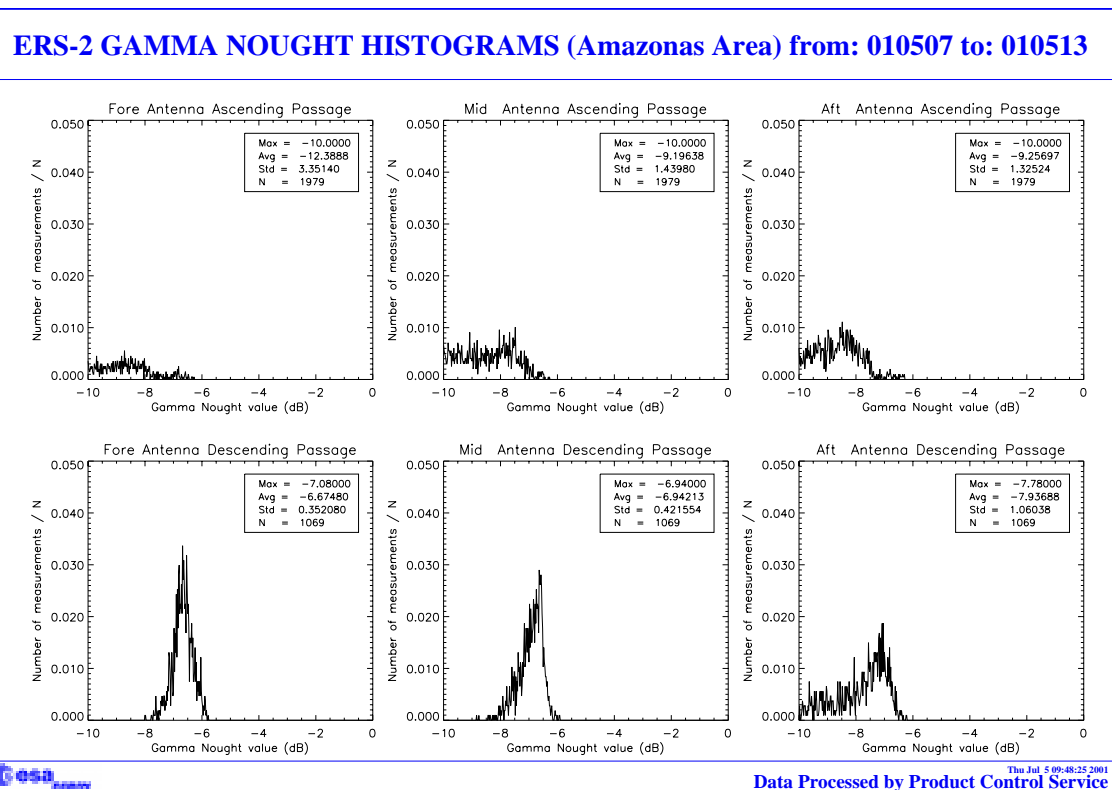
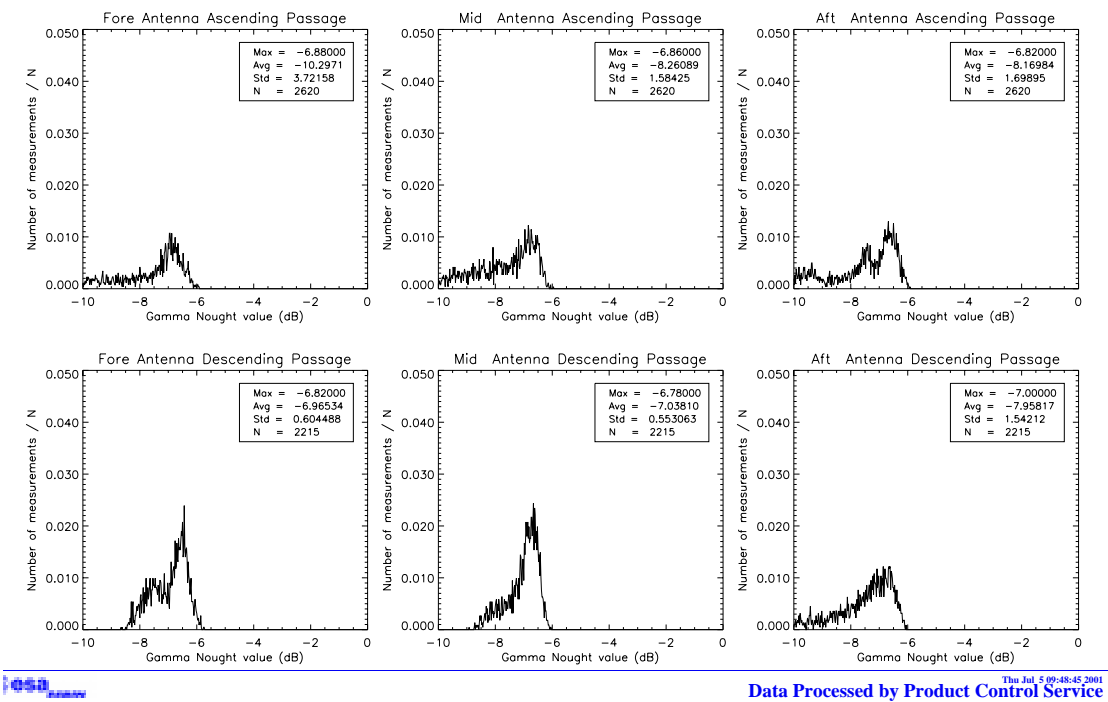


FIGURE 13. Gamma-nought histograms over Brazilian rain forest: third week of the cycle 63.

**ERS-2 GAMMA NOUGHT HISTOGRAMS (Amazonas Area) from: 010514 to: 010520**



**FIGURE 14. Gamma-nought histograms over Brazilian rain forest: fourth week of the cycle 63.**

**ERS-2 GAMMA NOUGHT HISTOGRAMS (Amazonas Area) from: 010521 to: 010527**

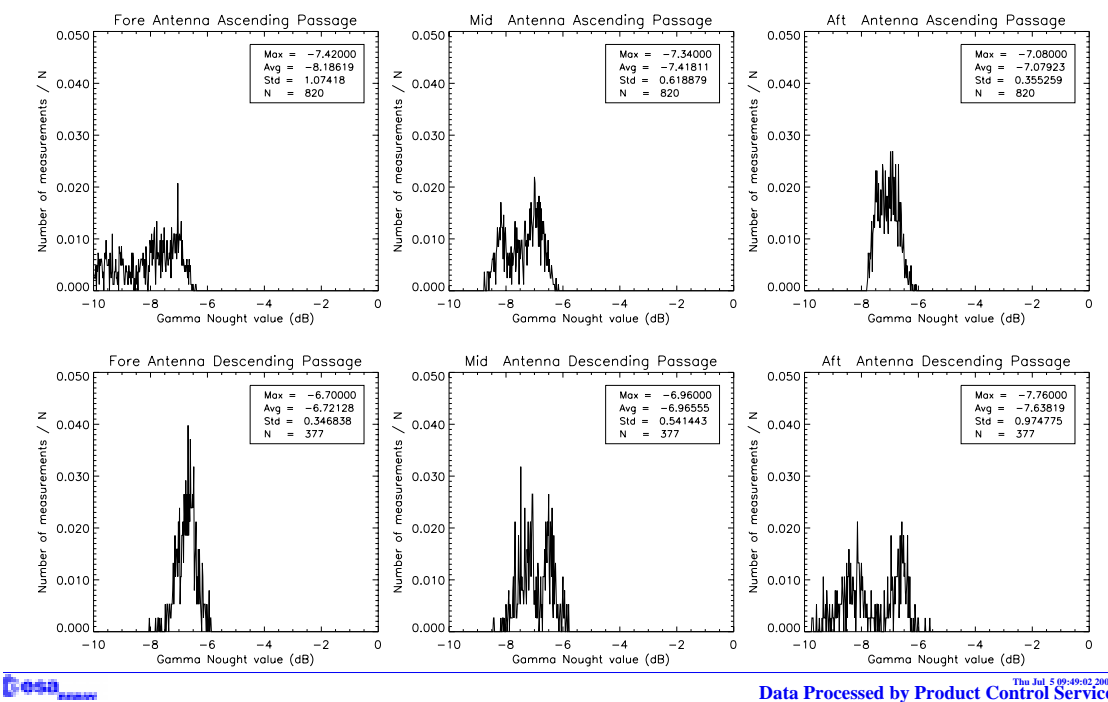


**FIGURE 15. Gamma-nought histograms over Brazilian rain forest: fifth week of the cycle 63**

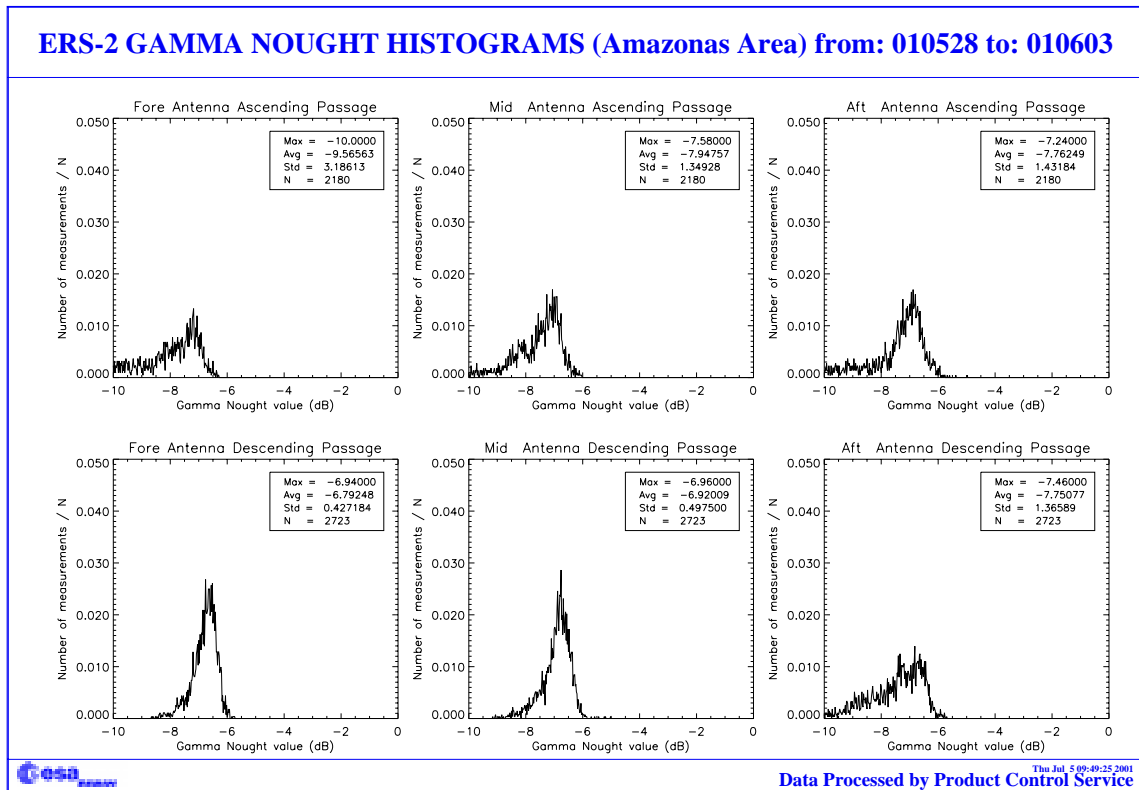


FIGURE 16. Gamma-nought histograms over Brazilian rain forest: first week of the cycle 64.

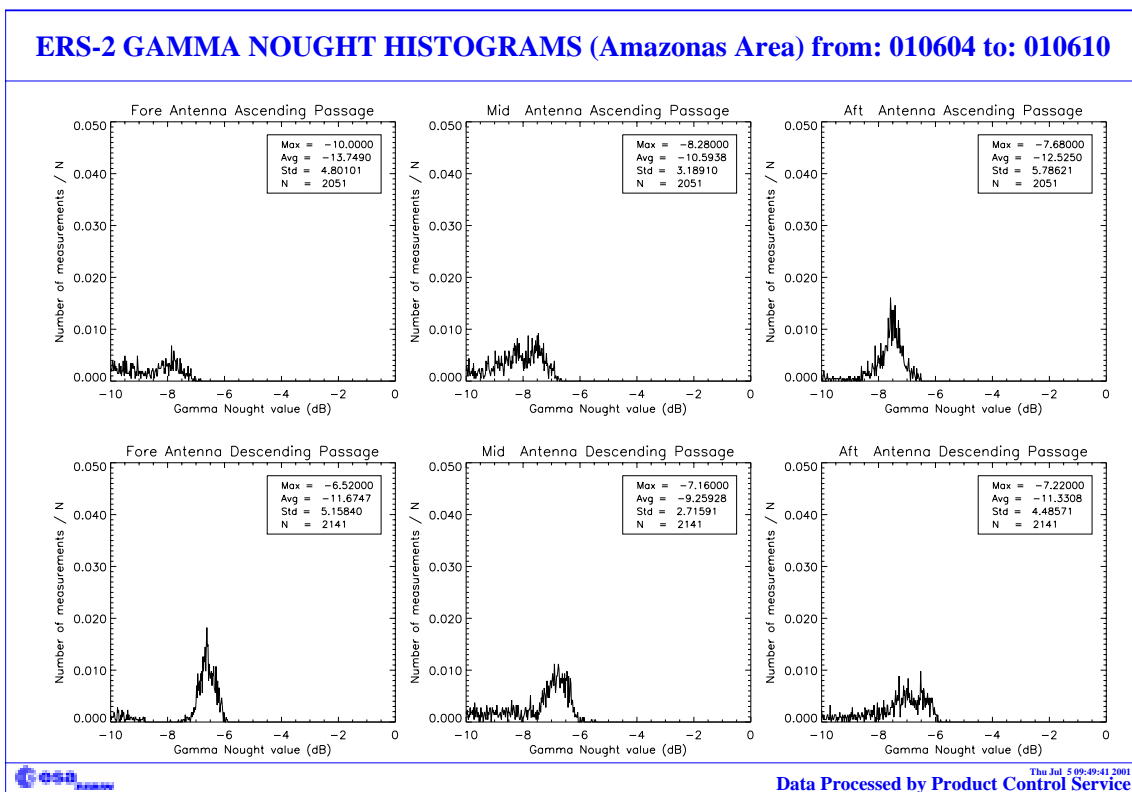


FIGURE 17. Gamma-nought histograms over Brazilian rain forest: second week of the cycle 64.

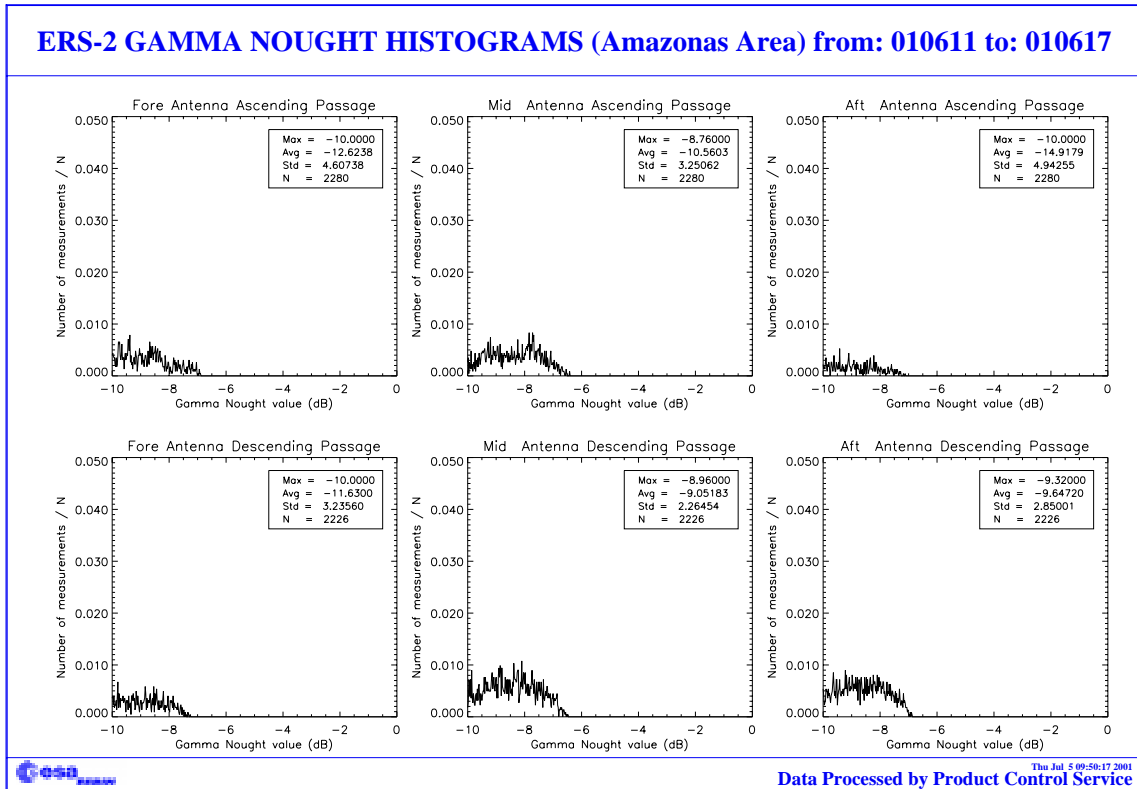


FIGURE 18. Gamma-nought histograms over Brazilian rain forest: third week of the cycle 64.

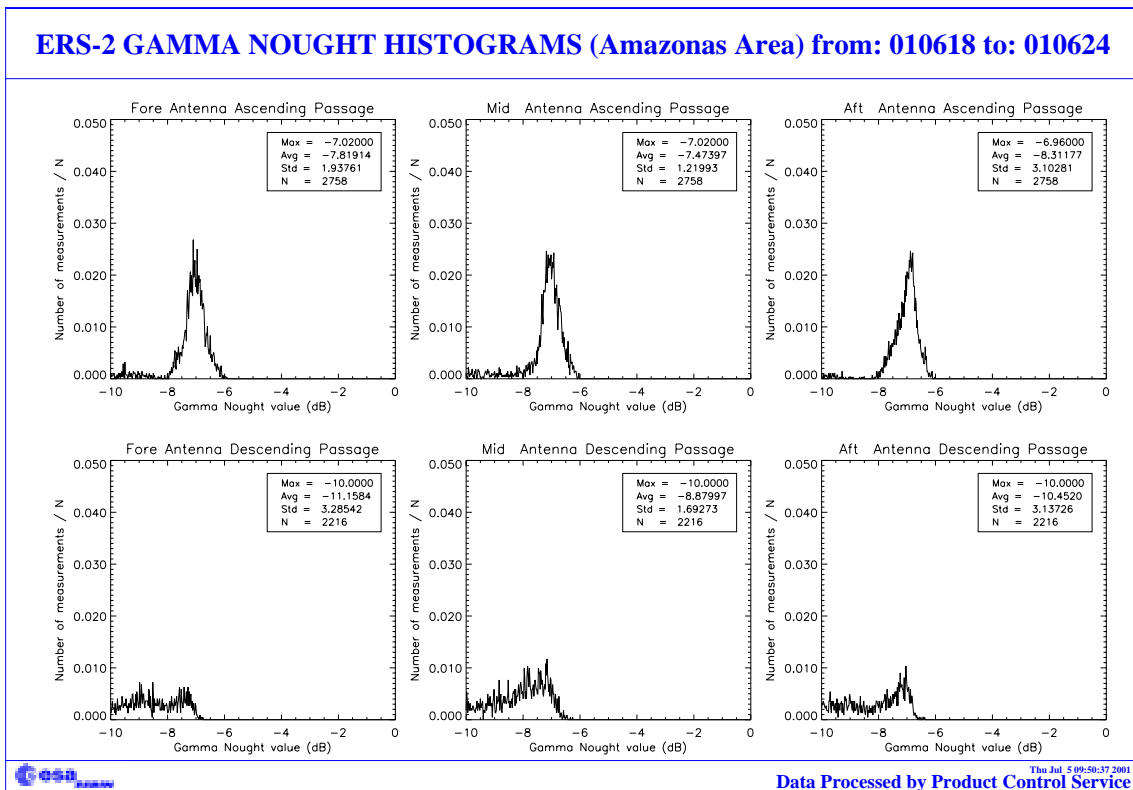
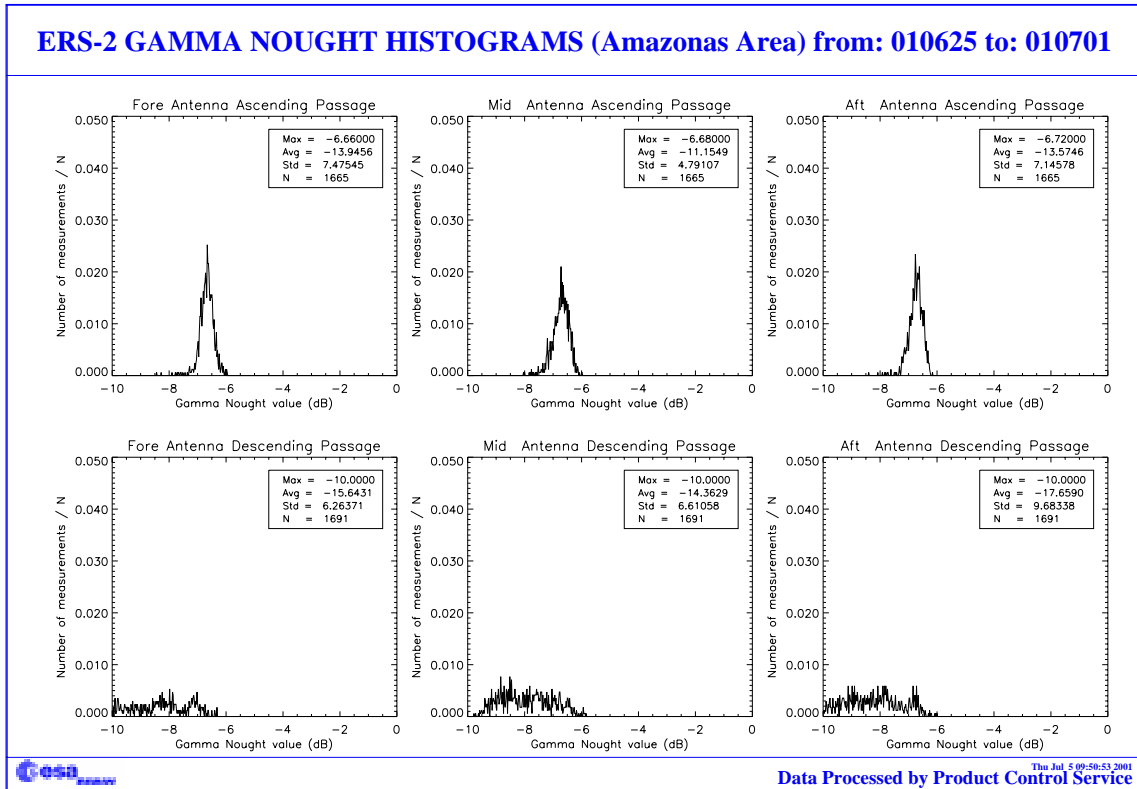


FIGURE 19. Gamma-nought histograms over Brazilian rain forest: fourth week of the cycle 64.



**FIGURE 20. Gamma-nought histograms over Brazilian rain forest: fifth week of the cycle 64.**

### 2.3.4 Gamma nought image of the reference area

The Figures 21 and 22 show maps of the gamma nought over the Brazilian rain forest. This is the area where statistics were computed. Each map has a resolution of 0.5 degrees in latitude and 0.5 degrees in longitude, roughly this is the instrument resolution at the latitude of the test site. In each resolution cell falls the average of all the valid observations available during one cycle (35 days).

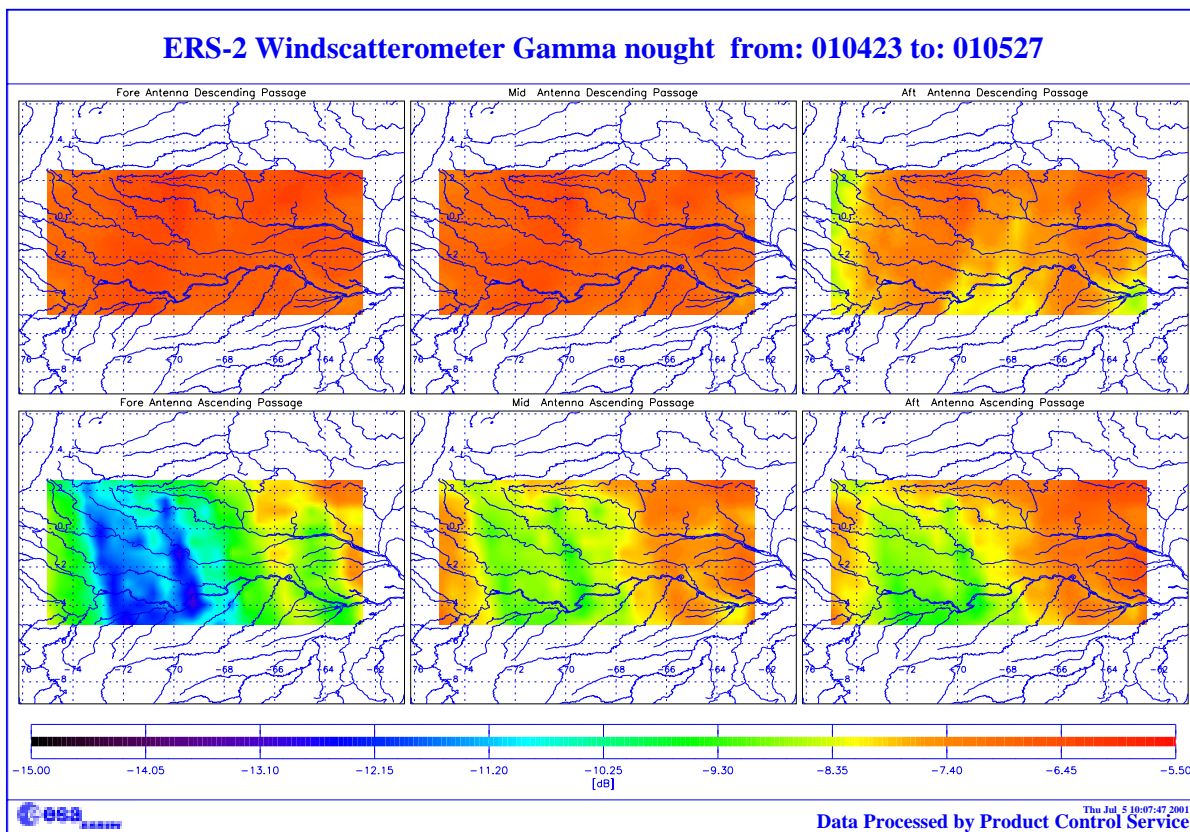


FIGURE 21. ERS-2 Scatterometer: gamma nought over the Brazilian rain forest cycle 63.

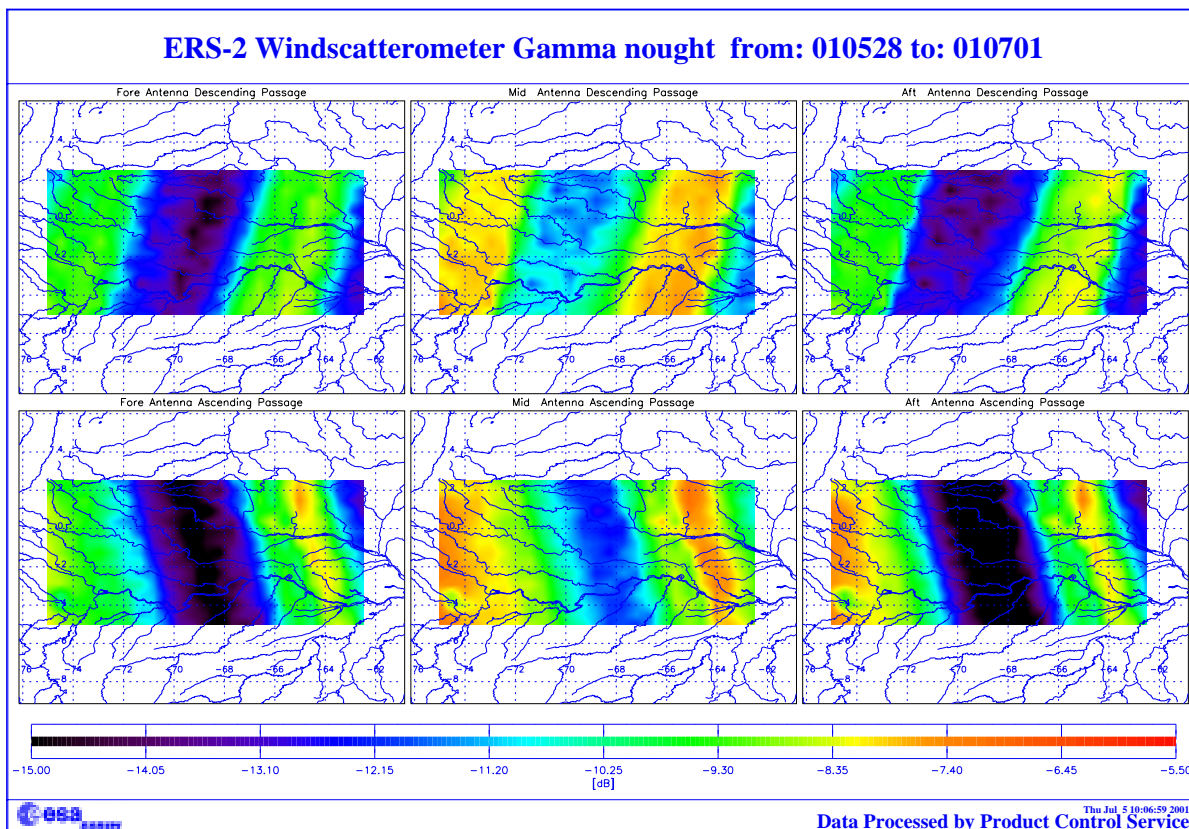


FIGURE 22. ERS-2 Scatterometer: gamma nought over the Brazilian rain forest cycle 64

Due to the EBM operations and ZGM commissioning phase the signal over the Rain Forest has a large fluctuation (see the histograms in the previous pages). **For that reason the colour scale of the image has been extend from -15dB to -5.5 dB.** The large differences in the backscattering are due to different satellite attitude among the various passes over the test area.

### 2.3.5 Sigma nought evolution

The Figures 23 and 24 show the evolution of the sigma nought over the reference area. The analysis is done per orbit and per node and the scope is to evaluate the stability of the sigma nought for each incidence angle. The relative tracks chosen are those where the number of valid measurements for each node (across track) is greater than 20.

The time series show a good correlation among the adjacent nodes (near and far range) and the stability, of the sigma nought, until 17<sup>th</sup> January 2001, ranges from 0.2 to 0.5 dB depending on the node.

After 17<sup>th</sup> January 2001 due to operations in EBM mode and ZGM commissioning phase the curves show a clear drop.

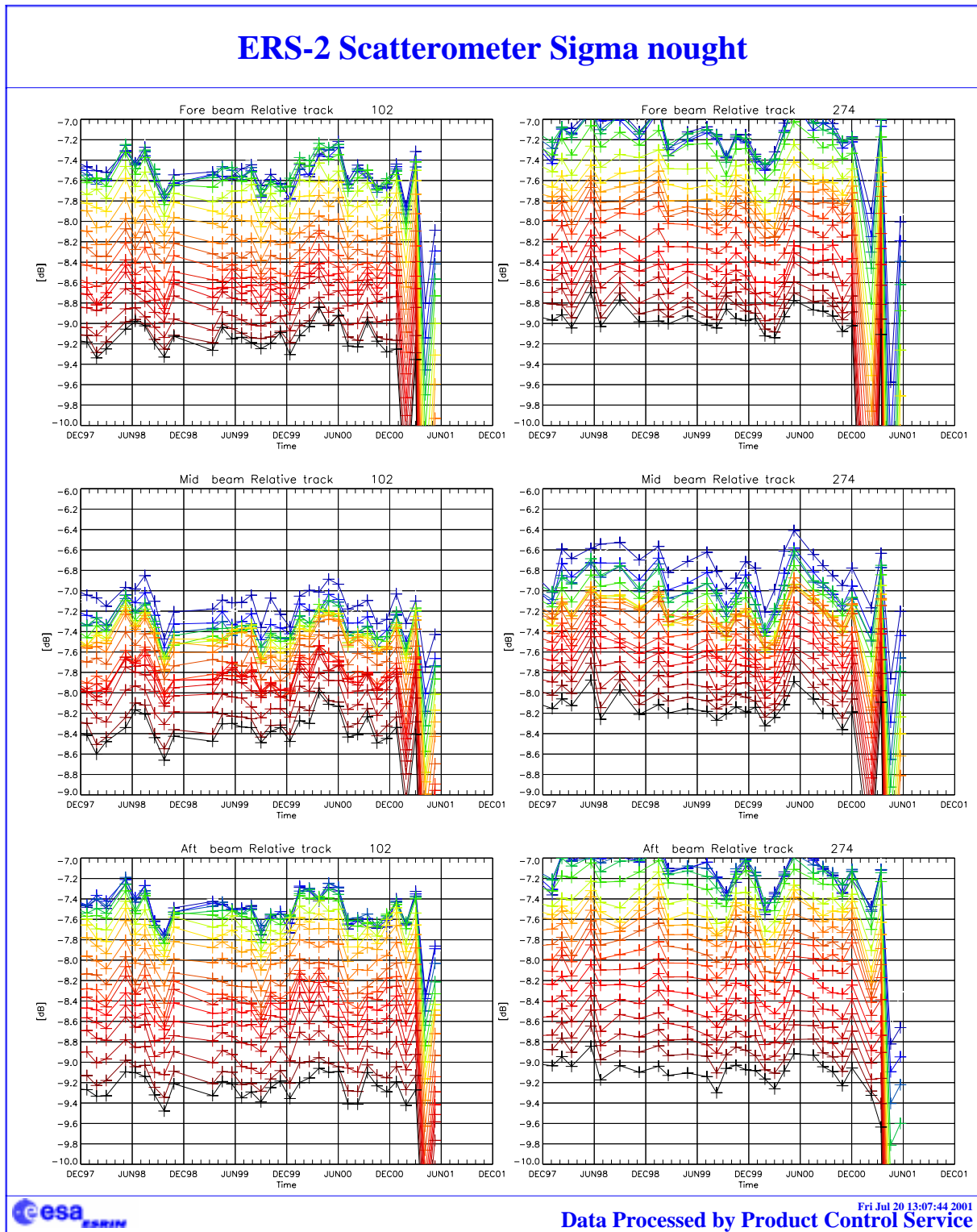


**FIGURE 23. Sigma nought over the test area: ascending passes relative tracks 102 (left panels) and 274 (right panels); all nodes across the swath (since December 1997).**

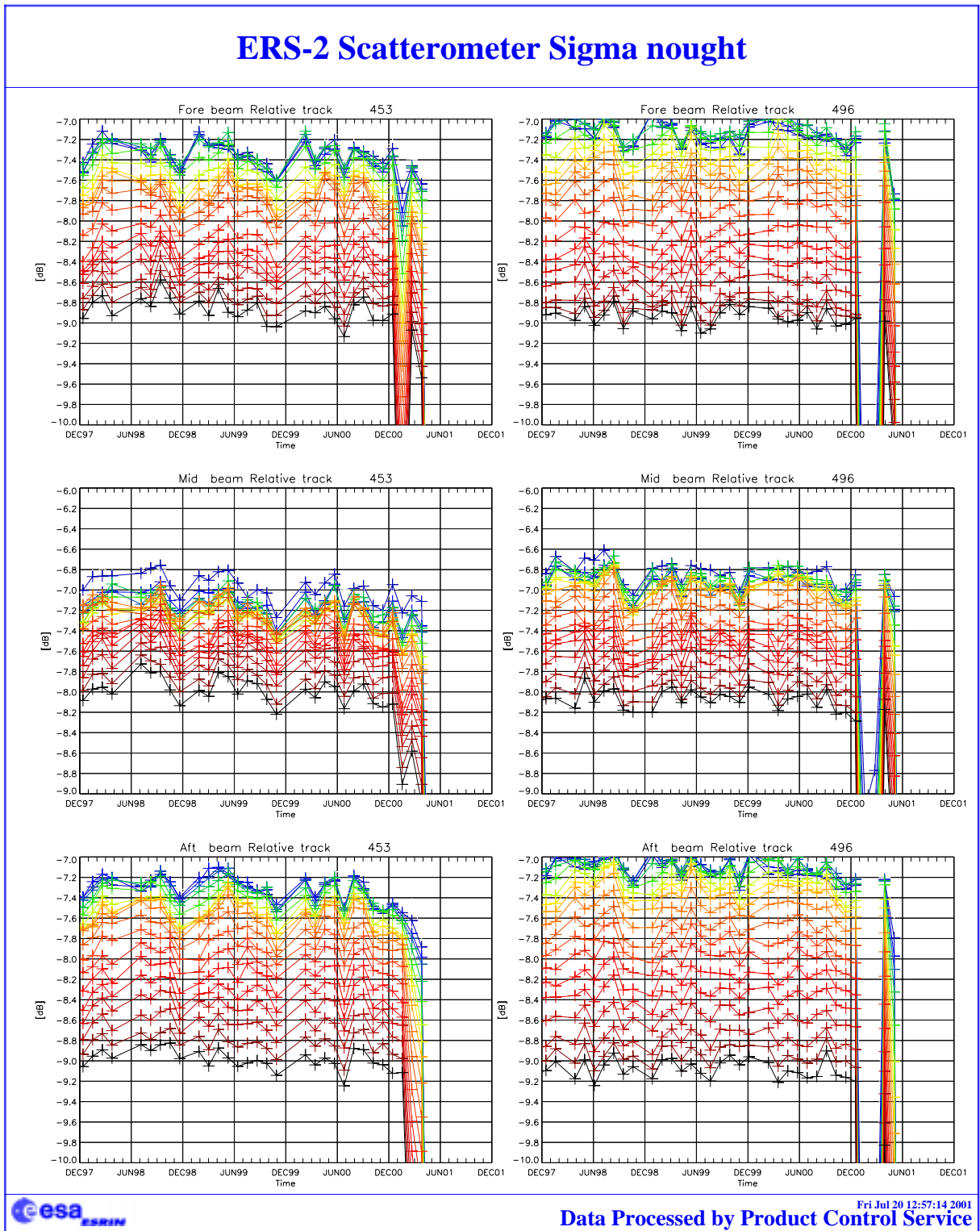


**FIGURE 24. Sigma nought over the test area: descending passes relative tracks 453 (left panels) and 496 (right panels); all nodes across the swath (since December 1997).**

### 2.3.6 Antenna temperature evolution over the Rain Forest

The monitoring of the antenna temperature over the Brazilian rain forest is performed by PCS. The antenna temperatures are retrieved from the satellite telemetry when the Scatterometer swath is over the test site and the instrument is active (AMI in wind only or wind/wave mode). The scope of this monitoring is to investigate a possible correlation between the antenna temperatures and the gamma-nought level. This correlation is not clear in the actual data because of the gamma nought variability over the selected area. A deep analysis is to be performed to better understand the facts.

The plots for the three beams and for the ascending, descending and all passes are presented in Figure 25. It is interesting to note that the annual variation is due to the earth inclination and that the antenna temperatures have an increase of roughly 1.0 degree per year in the case of the mid and fore antenna and 2 degrees per year for the aft antenna.

This temperature increase could be related to the degradation of the antennae protection film.

The result of the monitoring during the cycle 63 and cycle 64 shows that the antenna temperature evolution is as expected for the ascending passes. At the descending passes the seasonal increase of the antenna temperatures has a different behaviour for the Fore and Aft antenna. In particular during the cycle 64 the Fore antenna temperature had an increase of roughly 3 degrees during the descending passes. This could be related with the instability in the satellite attitude (change of the incidence angle between the antenna panel and the Sun light at the descending passes).

### ERS-2 WindScatterometer: Antennas Temperature Evolution Over Rain Forest

Data available for descending passes : 1079

Data available for ascending passes : 1180

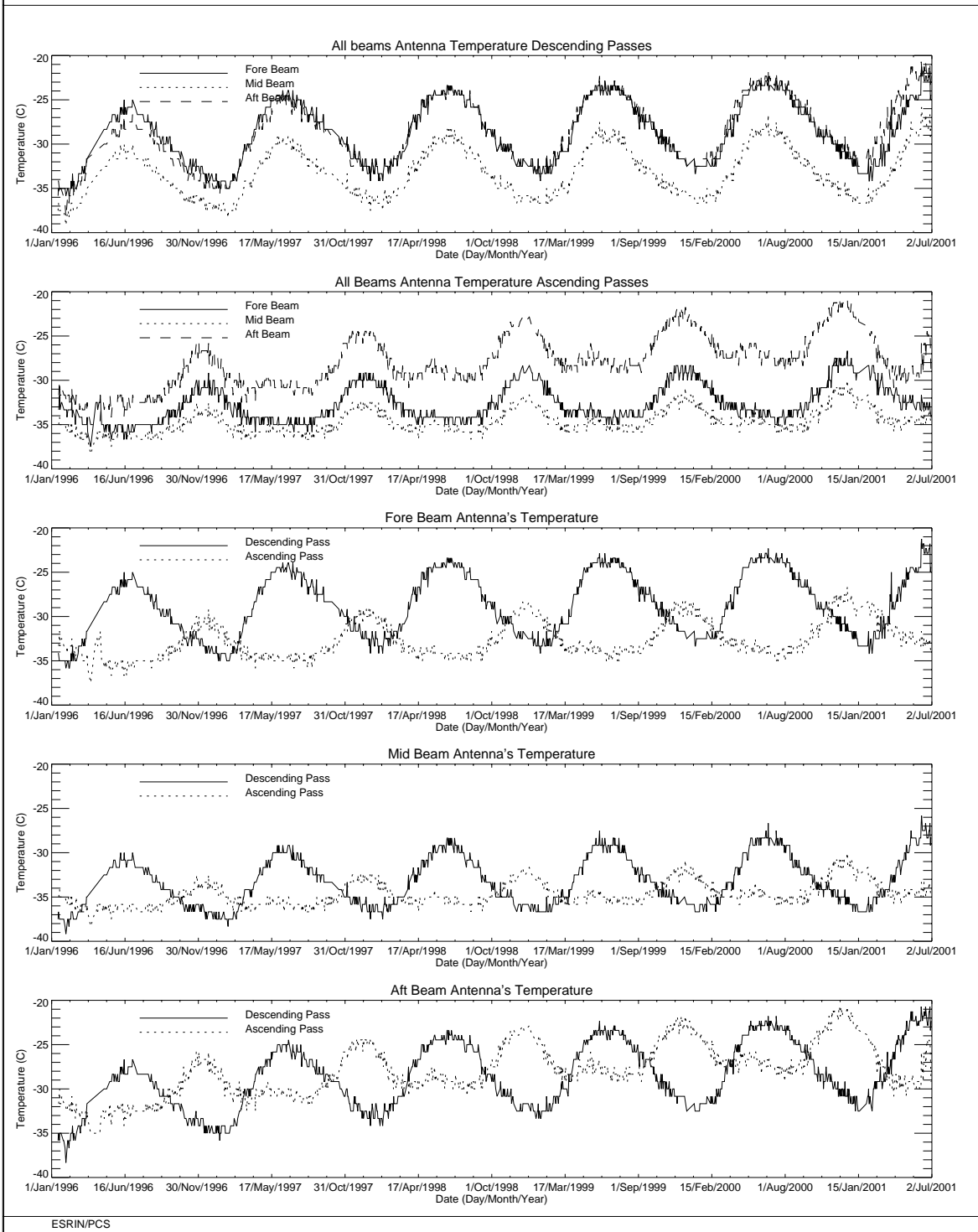


FIGURE 25. ERS-2 Scatterometer: evolution of the antenna temperatures over the Brazilian rain forest.

### **3.0 Instrument performance**

The instrument status is checked by monitoring the following parameters:

- Centre of Gravity (CoG) and standard deviation of the received signal spectrum. This parameter is useful for the monitoring of the orbit stability, the performances of the doppler compensation filter, the behaviour of the yaw steering mode and the performances of the devices in charge for the satellite attitude (e.g. gyroscopes, Earth sensor, Sun sensor).
- Noise power I and Q channel.
- Internal calibration pulse power.

the latter is an important parameter to monitor the transmitter and receiver chain, the evolution of pulse generator, the High Power Amplifier (HPA), the Travelling Wave Tube (TWT) and the receiver.

These parameters are extracted daily from the UWI products and averaged. The evolution of each parameter is characterised by a least square line fit. The coefficients of the line fit are printed in each plot.

#### **3.1 Centre of gravity and standard deviation of received power spectrum**

The Figure 26 shows the evolution of the two parameters for each beam.

The tendency from the beginning of the mission to the operation with the new Attitude On-board Control System (AOCS) configuration (7<sup>th</sup> February 2000) is a clear and regular increase of the Centre of gravity (CoG) of received spectrum for the three antennae. An increase of roughly 200 Hz was observed at the end of the AOCS qualification period. After the AOCS commissioning phase this parameter further evolved.

The old AOCS configuration (one Digital Earth Sensor - DES, one Digital Sun Sensor - DSS and 3 gyros) is no more considered safe because 3 of the six gyros on-board are out of order or very noisy. The new attitude control configuration is designed to pilot the ERS-2 using only one gyro plus the DES and the DSS modules. Scope of this new configuration is to extend the satellite lifetime by using the available gyros one at the time.

For the new AOCS configuration, the gyro 5 was used until 7<sup>th</sup> October 2000 when it failed. From 10<sup>th</sup> October 2000 to 24<sup>th</sup> October 2000 the gyro 6 was used. This explains the decrease of roughly 100Hz in the CoG of the received spectrum. From 25<sup>th</sup> October 2000 to 17<sup>th</sup> January 2001 the gyro 1 was used to pilot the ERS-2 satellite.

On 17<sup>th</sup> January 2001 the AOCS was upgraded. The new configuration allows to pilot the satellite without gyroscopes. Unfortunately a failure of the Digital Earth Sensor (DES A-side) caused ERS-2 to enter in Safe-Mode on the same day. On 25<sup>th</sup> January 2001 gyro #1 also failed. During the period of safe mode the spacecraft had drifted out of the nominal deadband by some 30 Km. The nominal orbit was reached on 6<sup>th</sup> February 2001.

In order to preserve the remaining gyroscopes for further manoeuvres, ERS-2 will now being operated in Extra Backup Mode (EBM). The EBM is a coarse attitude control mode. An upgrade of EBM has been performed on 30<sup>th</sup> March 2001. The aim of the upgrade was to introduce the Yaw steering law inside the piloting function. The new configuration has been renamed as EBM-YSM.

Since 7<sup>th</sup> June 2001 a new AOCS configuration is active on board. The purpose of the Zero Gyro Mode (ZGM) is to improve the yaw performances without use of gyroscope. The new configuration is under validation by ESOC-ASTRIUM-ESRIN.

Until 17<sup>th</sup> January 2001 the evolution of the standard deviation of the CoG of the received spectrum was stable apart from the change occurred on 26<sup>th</sup>, October 1998. On October 26<sup>th</sup>, 1998 the standard deviation of the CoG had, on average, a decrease of roughly 100 Hz for the fore and aft antenna and of roughly 30Hz for the mid antenna. This change is linked with the increase of the transmitted power (see Section 3.3).

Others changes in the AOCS configuration are recognised in Figure 26. The two steps observed at the beginning of the plots of the CoG (see Figure 19) are due to a change in the pointing subsystem (DES reconfiguration) side B instead of side A after a depointing anomaly (see table 2 for the list of the all AOCS depointing anomaly occurred during the ERS-2 mission). The first change is from 24<sup>th</sup>, January 1996 to 14<sup>th</sup>, March 1996, the second one is from 14<sup>th</sup> February 1997 to 22<sup>nd</sup> April 1997. During these periods side B was switched on. It is important to note that during the first time a clear difference in the CoG of the received spectrum is present only for the Fore antenna (an increase of roughly 100 Hz) while during the second time the change has affected all the three antennae (roughly an increase of 200 Hz, 50 Hz and 50 Hz for the fore, mid and aft antenna respectively).

**Table 2: ERS-2 Scatterometer AOCS depointing anomaly**

| From                                     | To                                       |
|--|--|
| 24 <sup>th</sup> January 1996 9:10 a.m.  | 26 <sup>th</sup> January 1996 6:53 p.m   |
| 14 <sup>th</sup> February 1997 1:25 a.m. | 15 <sup>th</sup> February 1997 3:44 p.m  |
| 3 <sup>rd</sup> June 1998 2:43 p.m.      | 6 <sup>th</sup> June 1998 12:47 a.m.     |
| 1 <sup>st</sup> September 1999 8:50 a.m. | 2 <sup>nd</sup> September 1999 1:28 a.m. |
| 7 <sup>th</sup> October 2000 4:38 p.m.   | 10 <sup>th</sup> October 2000 4:49 p.m.  |
| 24 <sup>th</sup> October 2000 4:05 p.m.  | 25 <sup>th</sup> October 2000 12:05 p.m. |
| 17 <sup>th</sup> January 2001            | 6 <sup>th</sup> February 2001            |

The Figure 26 shows also when the satellite was operated in Fine Pointing Mode (FPM) in EBM, ZGM mode or the on-board doppler compensation was missing. These events are related with the large peaks in the CoG of the received spectrum plots (fore and aft antenna) and are listed in Table 3.

**Table 3: ERS-2 Scatterometer anomalies in the CoG fore and aft antenna**

| Date   | Reason   |
|--|--|
| 26 <sup>th</sup> and 27 <sup>th</sup> September 1996 | missing on-board doppler coefficient (after cal. DC converter test period) |

| Date   | Reason   |
|--|--|
| 6 <sup>th</sup> and 7 <sup>th</sup> June 1998          | no Yaw Steering Mode<br>(after depointing anomaly)                       |
| 2 <sup>nd</sup> and 3 <sup>rd</sup> December 1998      | missing on-board doppler coefficients<br>(after AMI anomaly 228)         |
| 16 <sup>th</sup> and 17 <sup>th</sup> February 2000    | Fine Pointing Mode (FPM)<br>(due to AOCS mono-gyro qualification period) |
| 14 <sup>th</sup> April 2000                            | Fine Pointing Mode (FPM)   |
| 30 <sup>th</sup> May 2000                              | Fine Pointing Mode (FPM)   |
| 5 <sup>th</sup> July 2000                              | Fine Pointing Mode (FPM) after instrument switch-on                      |
| 27 <sup>th</sup> September 2000                        | Fine Pointing Mode (FPM) to up-load AOCS software patch                  |
| 2 <sup>nd</sup> November 2000                          | Fine Pointing Mode (FPM)   |
| 5 <sup>th</sup> and 6 <sup>th</sup> December 2000      | Fine Pointing Mode (FPM) due to orbital manoeuvre                        |
| 6 <sup>th</sup> February - 30 <sup>th</sup> March 2001 | Extra Backup Mode (EBM) coarse attitude control                          |
| 30 <sup>th</sup> March 2001- 7th June 2001             | EBM-YSM gyro-less yaw steering mode                                      |
| 7 <sup>th</sup> June 2001 - onwards                    | ZGM commissioning phase  |

The peaks shown in the plot of mid beam standard deviation of the CoG of the received spectrum are linked to the satellite manoeuvres and AOCS depointing anomaly.

During the cycle 63 and cycle 64 the Doppler frequency monitoring confirms for the daily average of the CoG of the received spectrum a very large fluctuation due to EBM operations and ZGM commissioning phase (see Figure 27). **Note that the vertical scale of the plots has been extended to take into account the EBM operations.**

The daily average standard deviation of the CoG of the received spectrum shows a constant improvement during the ZGM commissioning phase. In fact the value decreases from 7000 Hz to 5200 Hz for the Fore and Aft antenna and from 6300 Hz to 5700 Hz for the Mid antenna. **Note that the vertical scale of the plots has been extended to take into account the EBM operations.**

In Figure 28 is plotted, with different colours, the three days averaged CoG of the received spectrum (mid antenna) as time function from the ascending node (time = 0). Each unit of the X axis is 5 seconds from the ascending node while the Y axis is the frequency in Hz. The curves are obtained by filtering the evolution of the CoG of the received spectrum throughout the orbit. **Note that the vertical scale in Figure 28 has been extend from +/- 1.5 KHz to +/- 3.0 KHz to take into account the EBM operations.**

From Figure 28 the Doppler frequency (MID Antenna) has very large variation (above +/- 3 KHz) starting with the ZGM commissioning phase. For the operations in EBM (before 7th June 2001) the monitoring shows a variation between +/- 2 KHz, as reported for the previous cycles.

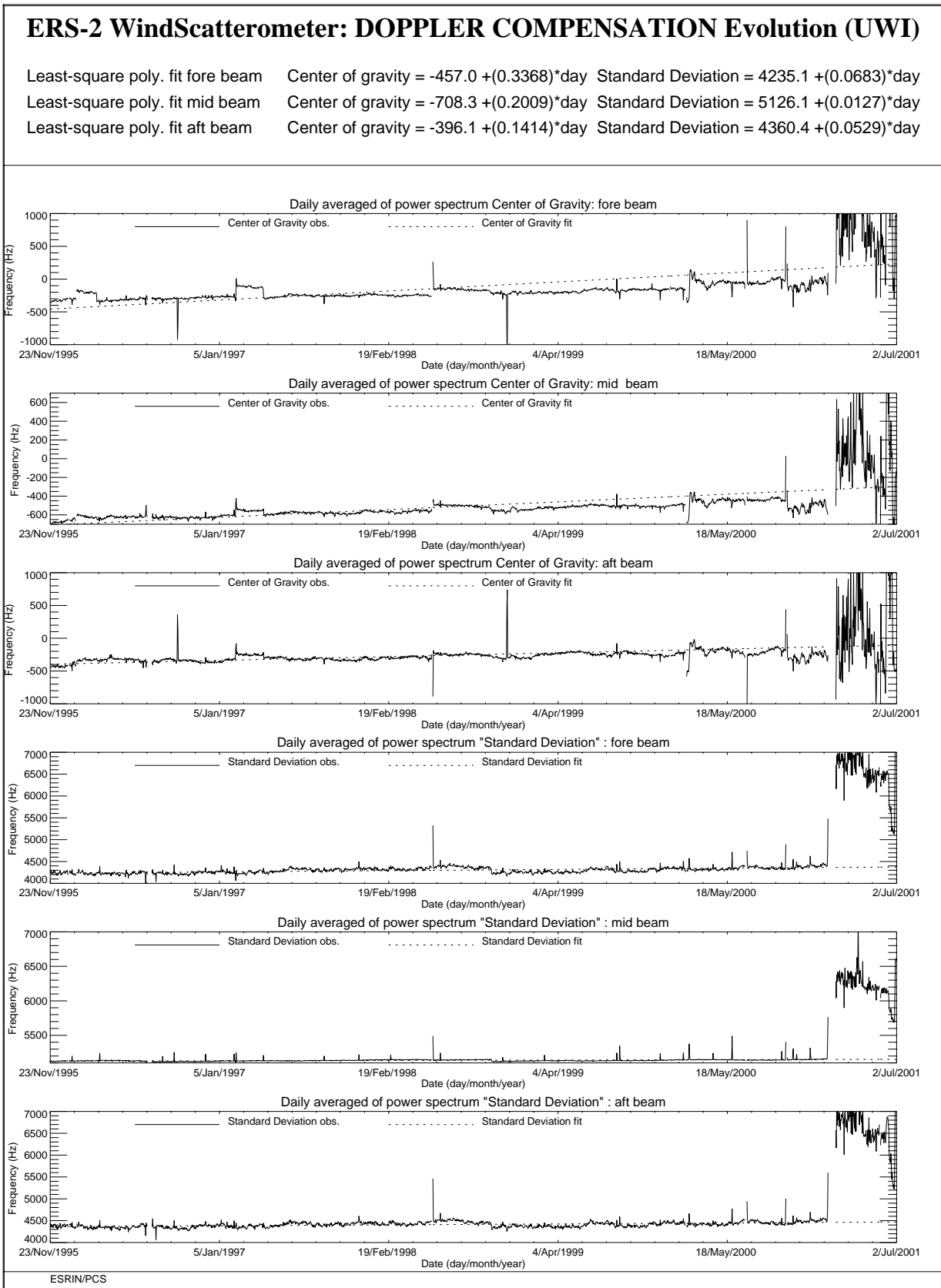


**FIGURE 26. ERS-2 Scatterometer: Centre of Gravity and standard deviation of received power spectrum since the beginning of the mission.**

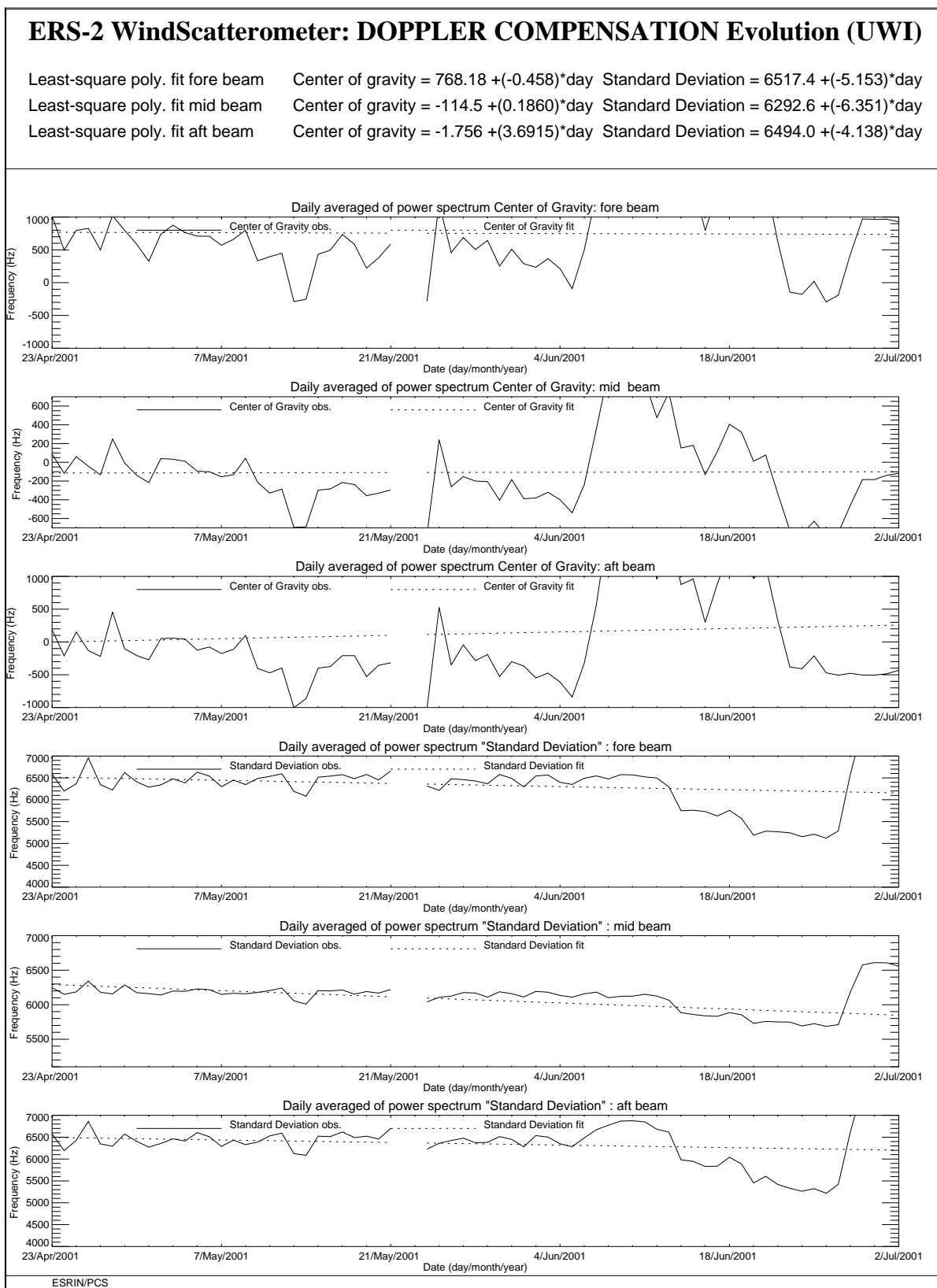


**FIGURE 27. ERS-2 Scatterometer: Centre of Gravity and standard deviation of received power spectrum during the cycle 63 and cycle 64.**

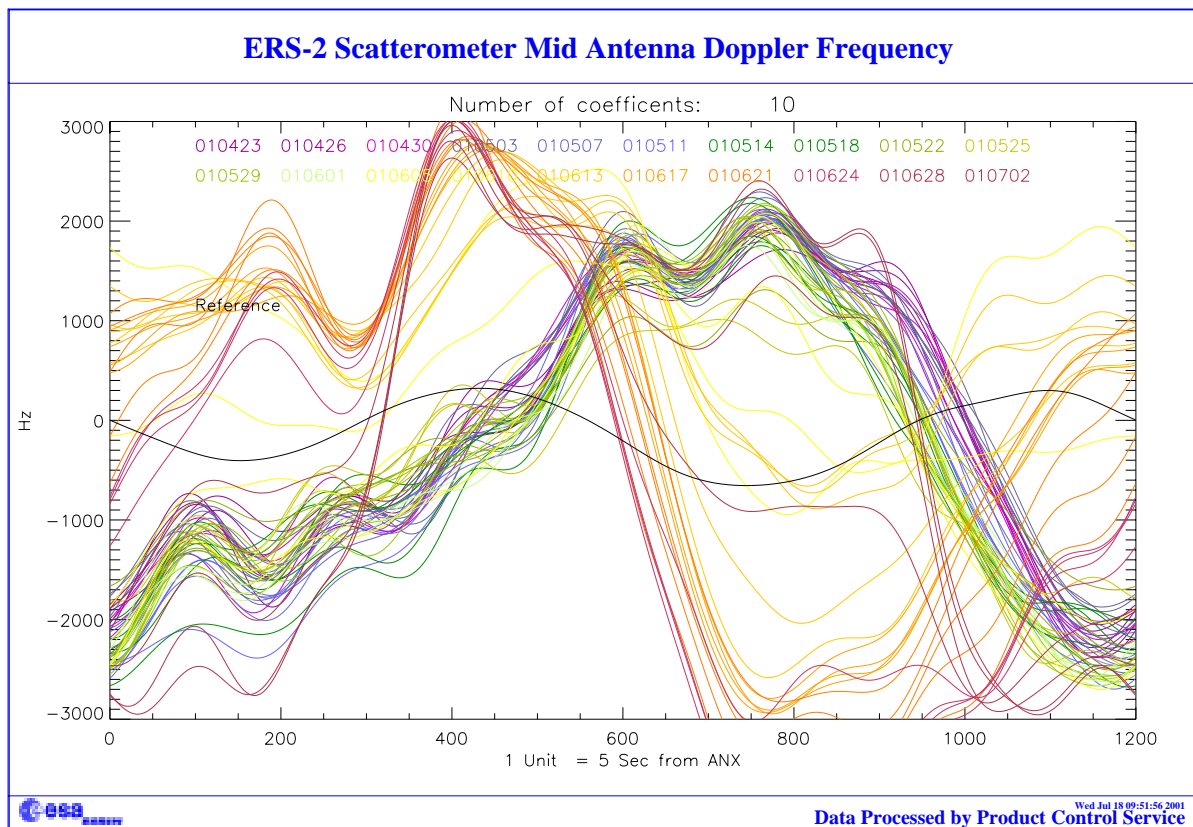


**FIGURE 28.** Low pass filtered evolution of the Mid beam CoG as function of ascending node time (1 unit 5 s.) Cycle 63 and cycle 64.

### 3.2 Noise power level I and Q channel

The results of the monitoring are shown in Figure 29. The first set of three plots presents the noise power evolution for the I channel while the second set shows the Q channel. The noise level is less than 1 ADC Unit for the fore and aft signals and is negligible for the mid one. From the plots one can see that the noise level is more stable in the I channel than in the Q one. The PCS suspects that an explanation should be found in the different position of the receivers, in particular it seems that the Q one is closer to the ATSR-GOME electronics. A confirmation of this hypothesis has been asked to ESTEC.

Since 5<sup>th</sup> December 1997 some high peaks appear in the plots. These high values for the daily mean are due to the presence for these special days of a single UWI product with an unrealistic value in the noise power field of its Specific Product Header. The analysis of the raw data used to generate these products lead in all cases to the presence of one source packet with a corrupted value in the noise field stored into the source packet Secondary Header. Table 4 presents the list of the UWI products affected by a corrupted noise field and disseminated during cycle 63 and cycle 64.

**Table 4: UWI products with noise field corrupted (cycle 63 and cycle 64)**

| Noise Field corrupted | Noise value (ADC Unit) | Acquisition Time |
|-----------------------|------------------------|------------------|
| None                  | -                      | -                |

The reason why noise field corruption is beginning from 5<sup>th</sup> December 1997 is at present unknown. It is interesting to note that at the beginning of December 1997, we started to get as well the corruption of the Satellite Binary Times (SBTs) stored in the EWIC product. The impact in the fast delivery products was the production of blank products starting from the corrupted EWIC until the end of the scheduled stop time. A change in the ground station processing in March 1998 overcame this problem.

Since 9<sup>th</sup> August 1998 some periods with a clear instability in the noise power have been recognised. Table 5 gives the detailed list.

**Table 5: ERS-2 Scatterometer instability in the noise power**

| From                           | To                             |
|--------------------------------|--------------------------------|
| 9 <sup>th</sup> August 1998    | 26 <sup>th</sup> October 1998  |
| 29 <sup>th</sup> November 1998 | 6 <sup>th</sup> December 1998  |
| 23 <sup>rd</sup> December 1998 | 24 <sup>th</sup> December 1998 |
| 7 <sup>th</sup> June 1999      | 10 <sup>th</sup> June 1999     |
| 17 <sup>th</sup> August 1999   | 22 <sup>nd</sup> August 1999   |
| 8 <sup>th</sup> September 1999 | 9 <sup>th</sup> September 1999 |
| 3 <sup>rd</sup> October 1999   | 8 <sup>th</sup> October 1999   |
| 16 <sup>th</sup> October 1999  | 18 <sup>th</sup> October 1999  |

| From                           | To                             |
|--------------------------------|--------------------------------|
| 26 <sup>th</sup> October 1999  | 28 <sup>th</sup> October 1999  |
| 25 <sup>th</sup> December 1999 | 2 <sup>nd</sup> January 2000   |
| 10 <sup>th</sup> February 2000 | 11 <sup>th</sup> February 2000 |
| 19 <sup>th</sup> March 2000    | 26 <sup>th</sup> March 2000    |

To better understand the instability of the noise power the PCS has carried out investigations in the scatterometer raw data (EWIC) to compute the noise power with more resolution. The result is that for the orbits affected by the instability the noise power had a decrease of roughly 0.7 dB for the fore and aft signals and a decrease of roughly 0.6 dB in the mid beam case (see the report for the cycle 42).

The decrease of the noise power during the orbits affected by the instability is comparable with the decrease of the internal calibration level that occurred during the same orbits. The reason of this instability (linked to the AMI anomalies) is still under investigation. A plot that shows the correlation among the noise power, the internal calibration level and the AMI anomaly is reported in section 3.3.

Figure 30 shows the evolution of the noise power since 26<sup>th</sup> October when 2 dB were added to the transmitted power. The periods with the instability in the noise power are clear shown in the plots in particular for the fore and aft beam signals.

During cycle 63 the monitoring of the noise power shows a stable result.

During the cycle 64 the monitoring of the noise (I and Q channel) shows a clear drop on 6<sup>th</sup> June 2001 (see Figure 30). The decrease of the noise power could be related with the starting of wave operation (for whole orbit) on that day.

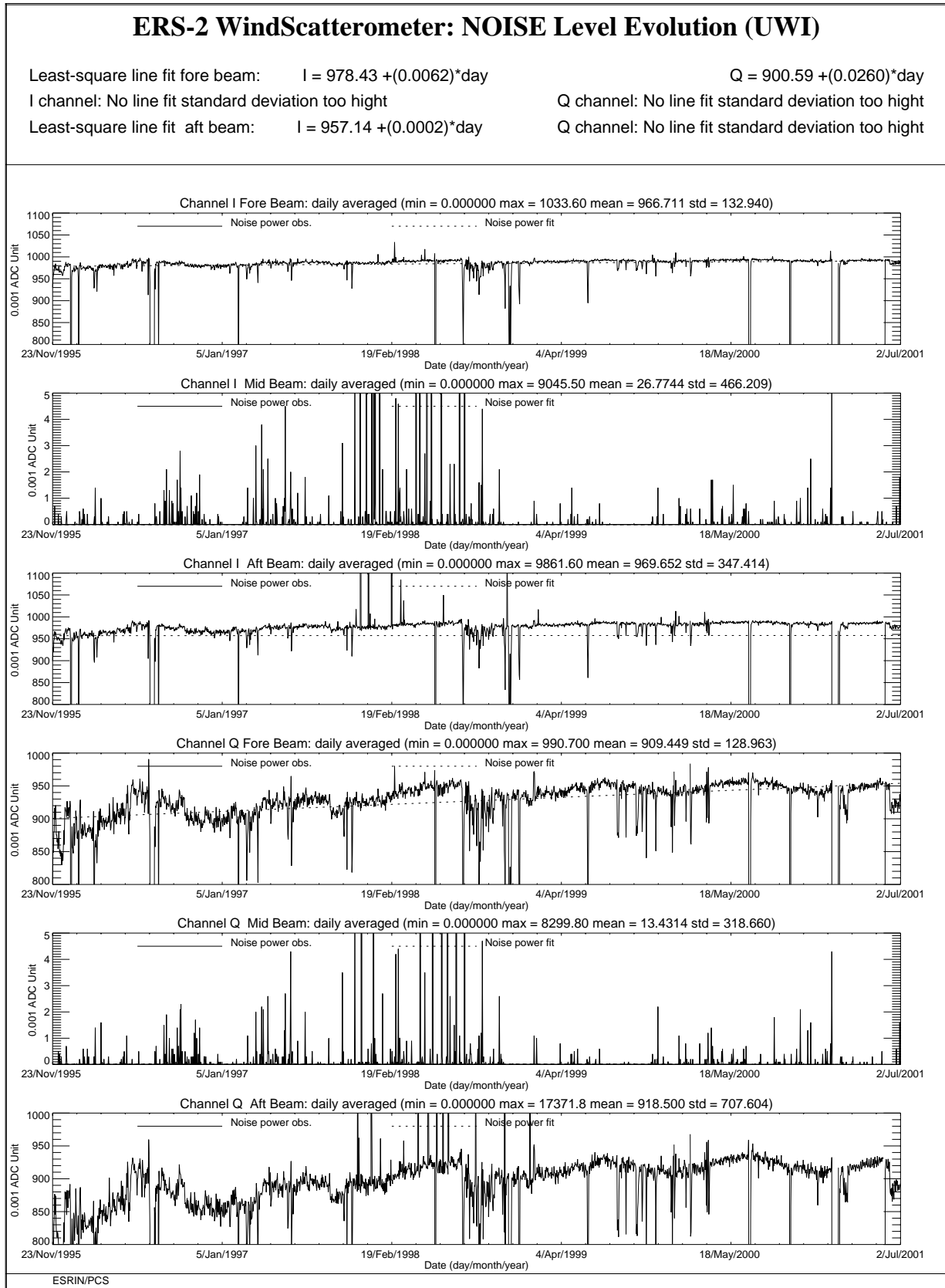
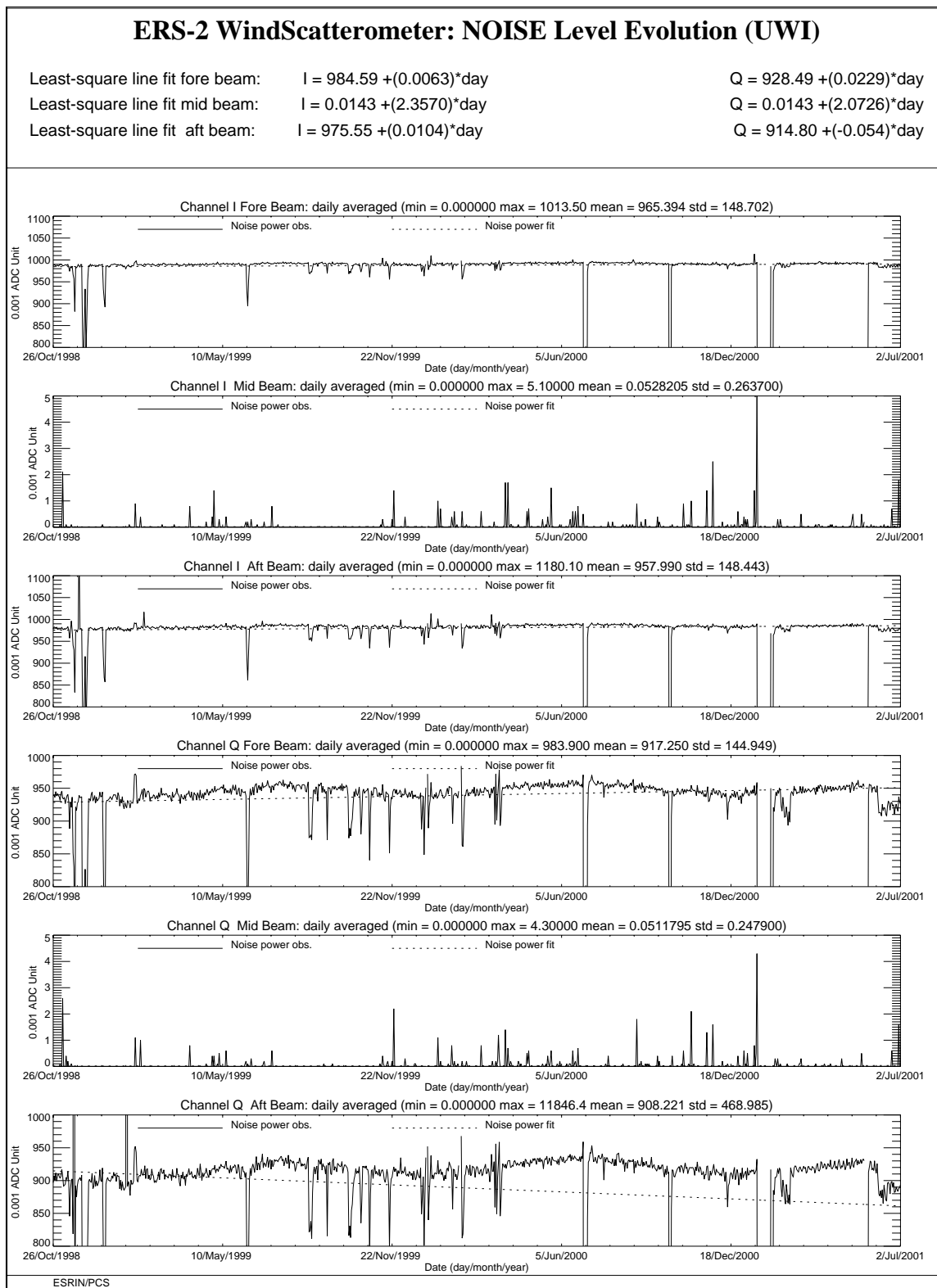


FIGURE 29. ERS-2 Scatterometer: noise power I and Q channel since the beginning of the mission.



**FIGURE 30. ERS-2 Scatterometer: noise power I and Q channel since 26<sup>th</sup> October 1998 when the transmitted power was increased by 2 dB.**

### 3.3 Power level of internal calibration pulse

For the internal calibration level, the results, since the beginning of the mission, are shown in Figure 32.

The high value of the variance in the fore beam until August, 12<sup>th</sup> 1996 is due to the ground processing. In fact all the blank source packets ingested by the processor were recognized as Fore beam source packets with a default value for the internal calibration level. The default value was applicable for ERS-1 and therefore was not appropriate for ERS-2 data processing. On August 12<sup>th</sup>, 1996 a change in the ground processing LUT overcame the problem.

Since the beginning of the mission a power decrease is detected. The power decrease is regular and affects the AMI when it is working in wind-only mode, wind/wave mode and image mode indifferently.

The reason is that the TWT is not working in saturation, so that a variation in the input signal is visible in the output. The variability of the input signal can be two-fold: the evolution of the pulse generator or the tendency of the switches between the pulse generator and the TWT to reset themselves into a nominal position. These switches were set into an intermediate position in order to put into operation the scatterometer instrument (on 16<sup>th</sup> November 1995).

After the change of the calibration subsystem on August 6<sup>th</sup>, 1996 the decrease is more evident and it is estimated in 0.09 dB per cycle (0.0025 dB/day).

On 26<sup>th</sup> October 1998 (cycle 37) to compensate for this decrease, 2.0 dB were added to the Scatterometer transmitted power and this explains the large step shows in Figure 31 and Figure 32. After that day the power decrease is on average 0.08 dB per cycle (0.0022 dB/day).

It is important to point out the efficiency of the internal calibration for keeping the absolute calibration level stable. In fact, no important change is noted in the monitoring of the gamma-nought level over the Brazilian rain forest during the power decrease and after the increase of the transmitted power (see section 2.0).

Since 9<sup>th</sup> August 1998 the internal calibration level shows an instability. This instability is very well correlated with the fluctuations observed in the noise power as outlined in section 3.2.

Figure 31 shows the daily average of the internal calibration and the noise power from 1<sup>st</sup> August 1998 to 2<sup>nd</sup> July 2001. In the figure are also reported the anomalies that affected the AMI and the platform (the triangles in the plot) and the days when the instability was very strong (asterisks in the plot).

From Figure 31 it seems that there is a clear correlation between the instability (noise and calibration level) and the AMI anomalies.

On 13<sup>th</sup> July 2000 an high peak (+3.5 dB) was detected in the transmitted power. This event has been investigated deeply by PCS and ESOC. The results of the analysis are reported in the technical note “ERS-2 Scatterometer: high peak in the calibration level” available in the PCS. The high transmitted power was obtained after an arc event which occurred inside the HPA. After that event the calibration level had an average increase of roughly 0.14 dB.

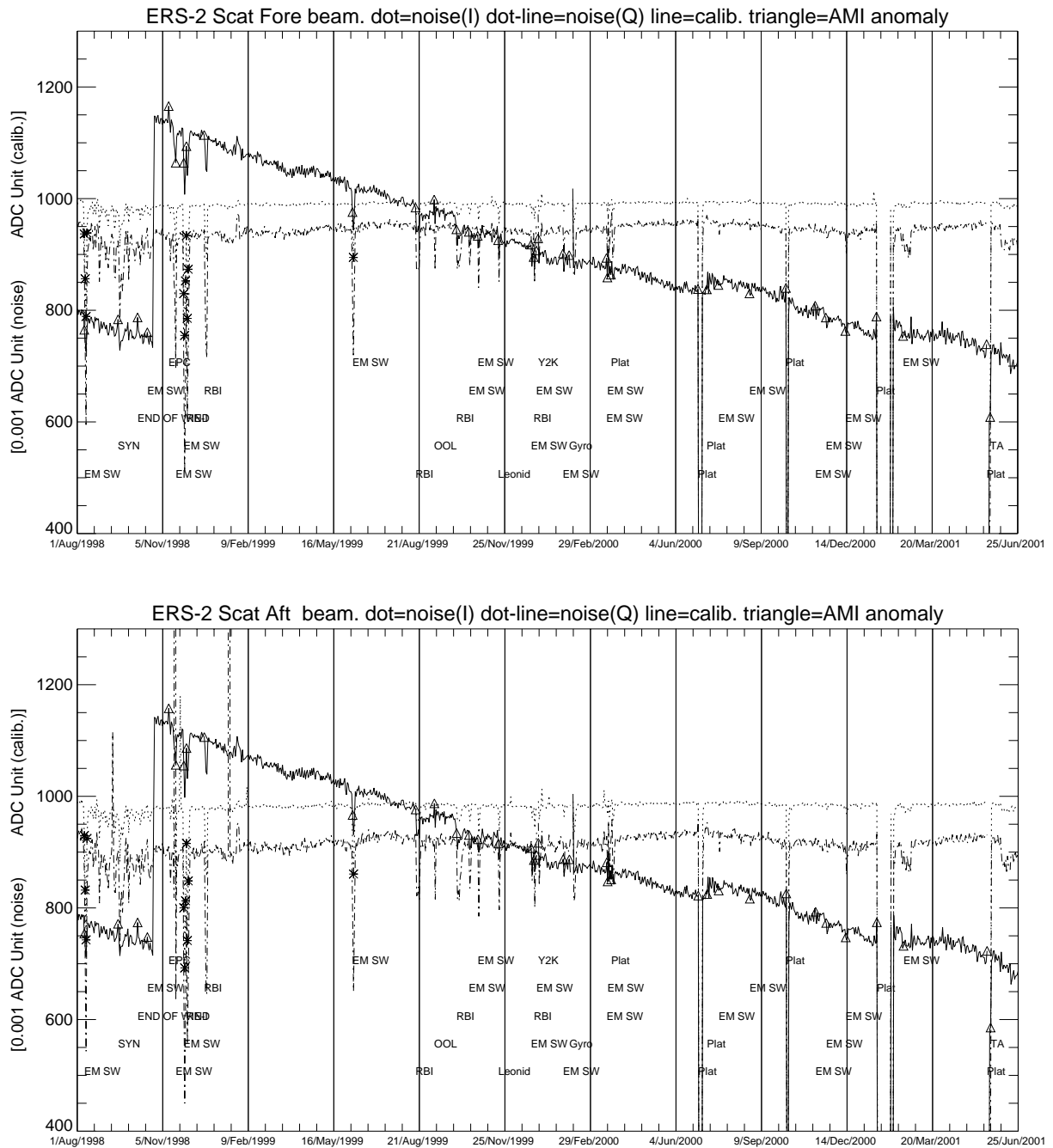
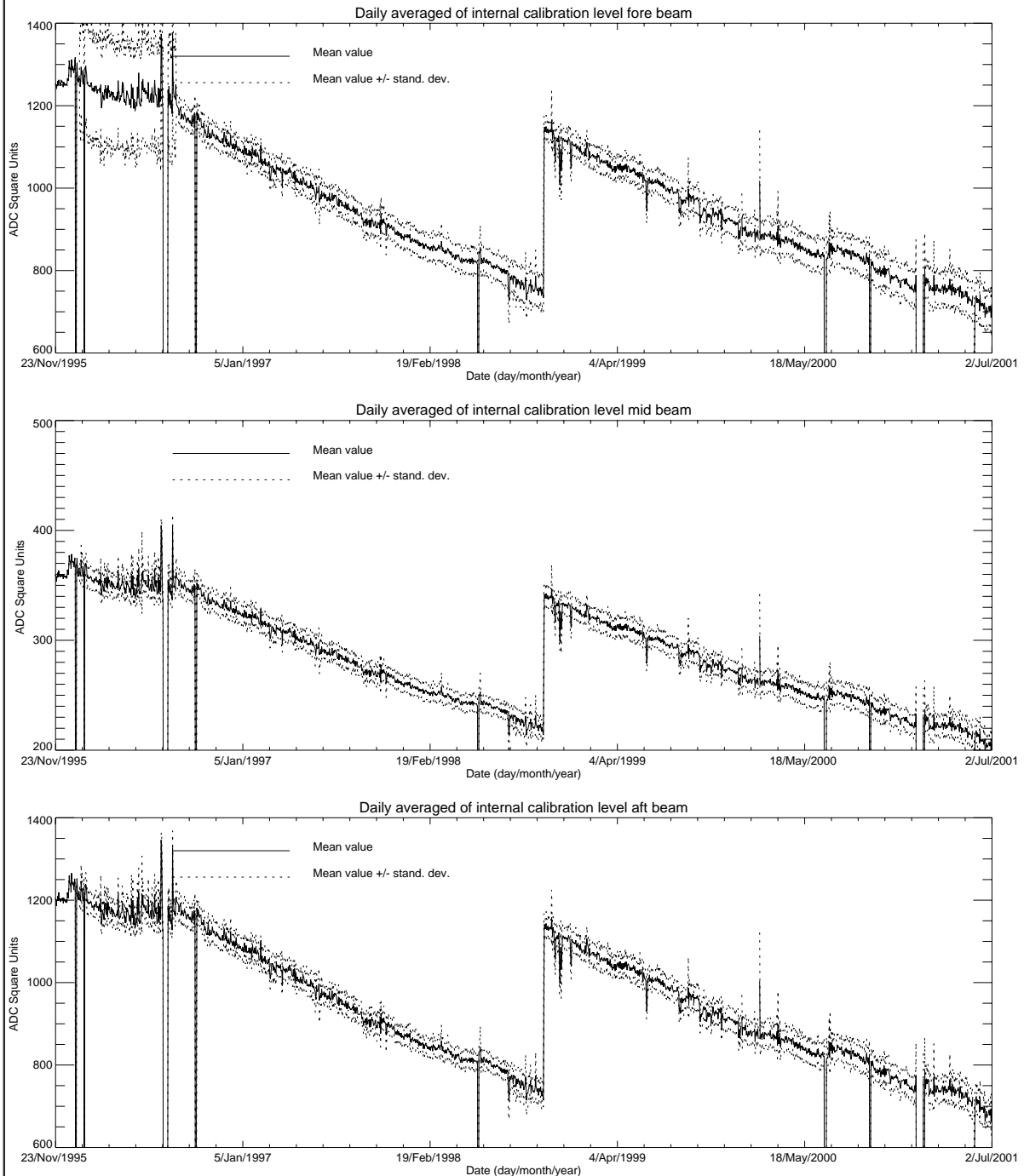


**FIGURE 31. ERS-2 Scatterometer: noise power (I and Q channel) and internal calibration power evolution from 1<sup>st</sup> August 1998 to 19<sup>th</sup> March 2001. Upper panel Fore antenna, lower panel Aft antenna.**

During the cycle 63 and cycle 64, on average, the power decrease was 0.18 dB/Cycle (see Figure 33). Therefore the previous zero trend is not confirmed and an on-board gain increase shall be planned. The actual level is roughly 0.36 dB below the level reached on October 1998.

### ERS-2 WindScatterometer: Internal CALIBRATION Level Evolution (UWI)

|                                       |                           |   |
|---------------------------------------|---------------------------|---|
| Least-square polynomial fit fore beam | gain (dB) per day -0.0002 | $977.191 + (-0.0392194) \cdot \text{day}$ |
| Least-square polynomial fit mid beam  | gain (dB) per day -0.0002 | $286.398 + (-0.0101728) \cdot \text{day}$ |
| Least-square polynomial fit aft beam  | gain (dB) per day -0.0002 | $959.035 + (-0.0364927) \cdot \text{day}$ |



ESRIN/PCS

FIGURE 32. ERS-2 Scatterometer: power of internal calibration pulse since the beginning of the mission.

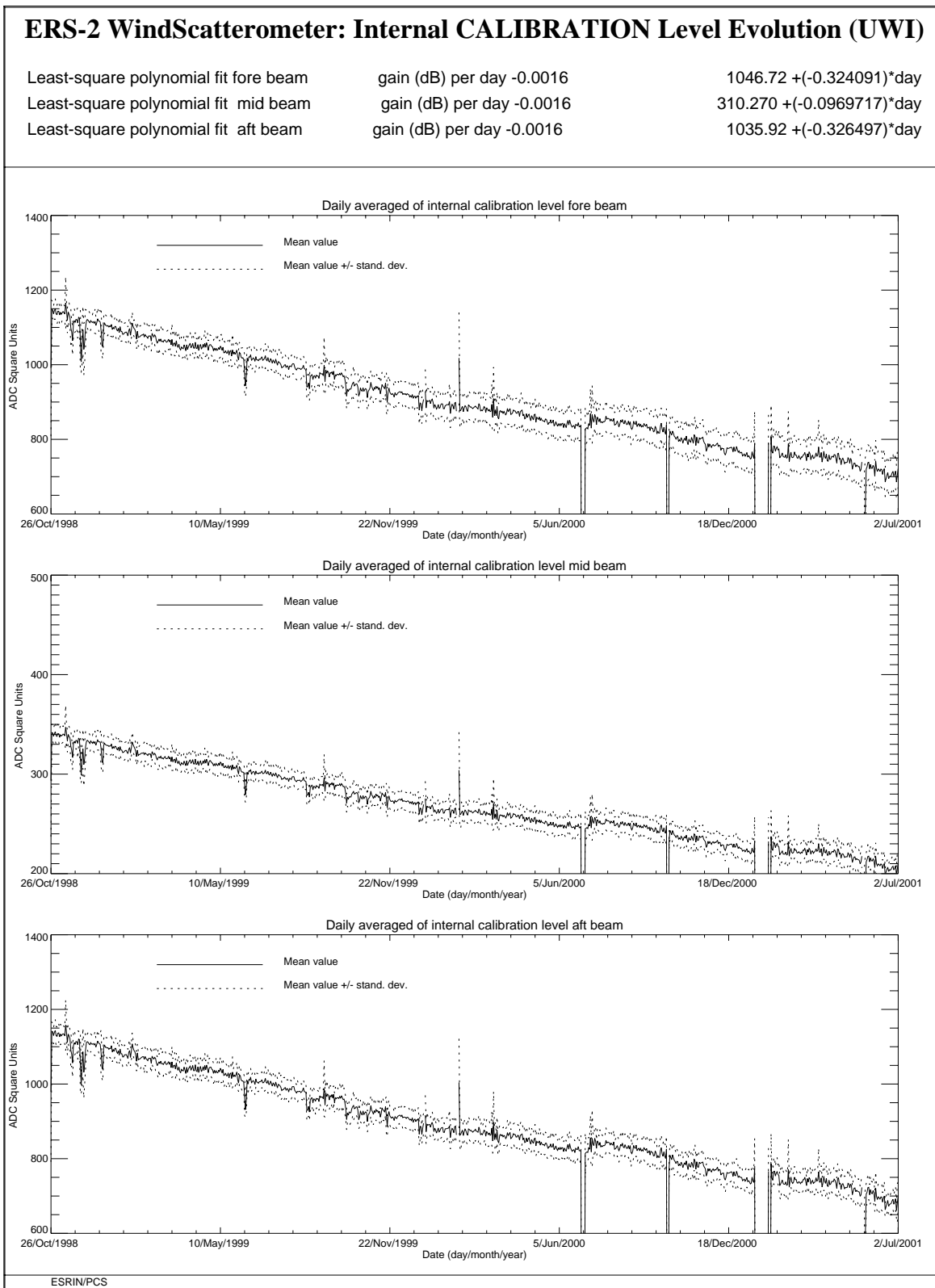


**FIGURE 33. ERS-2 Scatterometer: power of internal calibration level since 26<sup>th</sup> October 1998 when the transmitted power was increased by 2.0 dB.**

## 4.0 Products performance

One of the most important point in the monitoring of the products performance is their availability. The Scatterometer is a part of ERS payload and it is combined with a Synthetic Aperture Radar (SAR) into a single Active Microwave Instrument (AMI). The SAR users requirements and the constraints imposed by the on-board hardware (e.g. amount of data that can be recorded in the on-board tape) set rules in the mission operation plan.

The principal rules that affected the Scatterometer instruments are:

- over the Ocean the AMI is in wind/wave mode (scatterometer with small SAR imagettes acquired every 30 sec.) and the ATSR-2 is in low rate data mode.
- over the Land the AMI is in wind only mode (only scatterometer) and the ATSR-2 is in high rate mode. (Due to on board recorder capacity, ATSR-2 in high rate is not compatible with Sar wave imagette acquisitions.)

This strategy preserves the Ocean mission.

Moreover:

- the SAR images are planned as consequence of users' request.

These rules have an impact on the Scatterometer data availability as shown in Figure 34.

Each segment of the orbit has different colour depending on the instrument mode: brown for wind only mode, blue for wind-wave mode and green for image mode. The red and yellow colours correspond to gap modes (no data acquired). The major problems came from the orbit segments between Australia and Antarctic and between Africa and Antarctic where a lot of data are not acquired. A solution has been proposed by ESRIN. The new mission operation plan has not been accepted because it increase the number of AMI switches. As reported by ESTEC that increase has a negative impact in the instrument time life.

A new set of parameters in the Mission Plan Schedule (MPS) is operative from cycle 55 onwards. The new set allow the reduction of the gap mode when the AMI switches from wind/wave mode to wind\_only mode. The reduction of the gap mode is up to 30 seconds and depends on the track.

For cycle 63 the percentage of the ERS-2 AMI activity is shown in table 6. The increase of gap mode is due to the platform unavailability occurred from 22<sup>nd</sup> to 24<sup>th</sup> May 2001 and due to the instrument unavailability occurred on 25<sup>th</sup> May 2001.

**Table 6: ERS-2 AMI activity (cycle 63)**

| AMI modes          | ascending passes | descending passes |
|--------------------|------------------|-------------------|
| Wind and Wind-Wave | <b>87.8%</b>     | <b>82.9%</b>      |
| Image              | <b>1.8%</b>      | <b>5.8%</b>       |
| Gap and others     | <b>10.4%</b>     | <b>11.3%</b>      |

For the cycle 64 the percentage of ERS-2 AMI activity is shown in table 7. Since 6<sup>th</sup> June 2001, due to the ZGM commissioning phase, AMI instrument is operated in wind-wave mode throughout the whole orbit

**Table 7: ERS-2 AMI activity (cycle 64)**

| AMI modes          | ascending passes | descending passes |
|--------------------|------------------|-------------------|
| Wind and Wind-Wave | <b>94.1%</b>     | <b>90.5%</b>      |
| Image              | <b>1.8%</b>      | <b>5.5%</b>       |
| Gap and others     | <b>4.1%</b>      | <b>4.0%</b>       |

Table 8 reports the major data lost due to the test periods and AMI or satellite anomalies occurred after August 6<sup>th</sup>, 1996 (before that day for many times data were not acquired due to the DC converter failure).

**Table 8: ERS-2 Scatterometer mission major data lost after 6<sup>th</sup>, August 1996**

| Start date                        | Stop date                         | Reason   |
|-----------------------------------|-----------------------------------|--|
| September 23 <sup>rd</sup> , 1996 | September 26 <sup>th</sup> , 1996 | ERS-2 switched off due to a test period                |
| February 14 <sup>th</sup> , 1997  | February 15 <sup>th</sup> , 1997  | ERS-2 switched off due to a depointing anomaly         |
| June 3 <sup>rd</sup> , 1998       | June 6 <sup>th</sup> , 1998       | ERS-2 switched off due to a depointing anomaly         |
| November 17 <sup>th</sup> , 1998  | November 18 <sup>th</sup> , 1998  | ERS-2 switched off to face out Leonide meteo storm     |
| September 22 <sup>nd</sup> 1999   | September 23 <sup>rd</sup> 1999   | ERS-2 switched off due to Year 2000 certification test |
| November 17 <sup>th</sup> , 1999  | November 18 <sup>th</sup> , 1999  | ERS-2 switched off to face out Leonide meteo storm     |
| December 31 <sup>st</sup> , 1999  | January 2 <sup>nd</sup> , 2000    | ERS-2 switched off Y2K transition operation            |
| February 7 <sup>th</sup> , 2000   | February 9 <sup>th</sup> , 2000   | ERS-2 switched off due to new AOCS s/w up-link         |
| June 30 <sup>th</sup> , 2000      | July 5 <sup>th</sup> , 2000       | ERS-2 Payload switched-off after RA anomaly            |
| July 10 <sup>th</sup> , 2000      | July 11 <sup>th</sup> , 2000      | ERS-2 Payload reconfiguration                          |
| October 7 <sup>th</sup> , 2000    | October 10 <sup>th</sup> , 2000   | ERS-2 Payload switched-off after AOCS anomaly          |
| January 17 <sup>th</sup> , 2001   | February 5 <sup>th</sup> , 2001   | ERS-2 Payload switched-off due to AOCS anomaly         |
| May 22 <sup>nd</sup> , 2001       | May 24 <sup>th</sup> , 2001       | ERS-2 Payload switched-off due to platform anomaly     |
| May 25 <sup>th</sup> , 2001       | May 25 <sup>th</sup> , 2001       | AMI switched-off due thermal analysis                  |

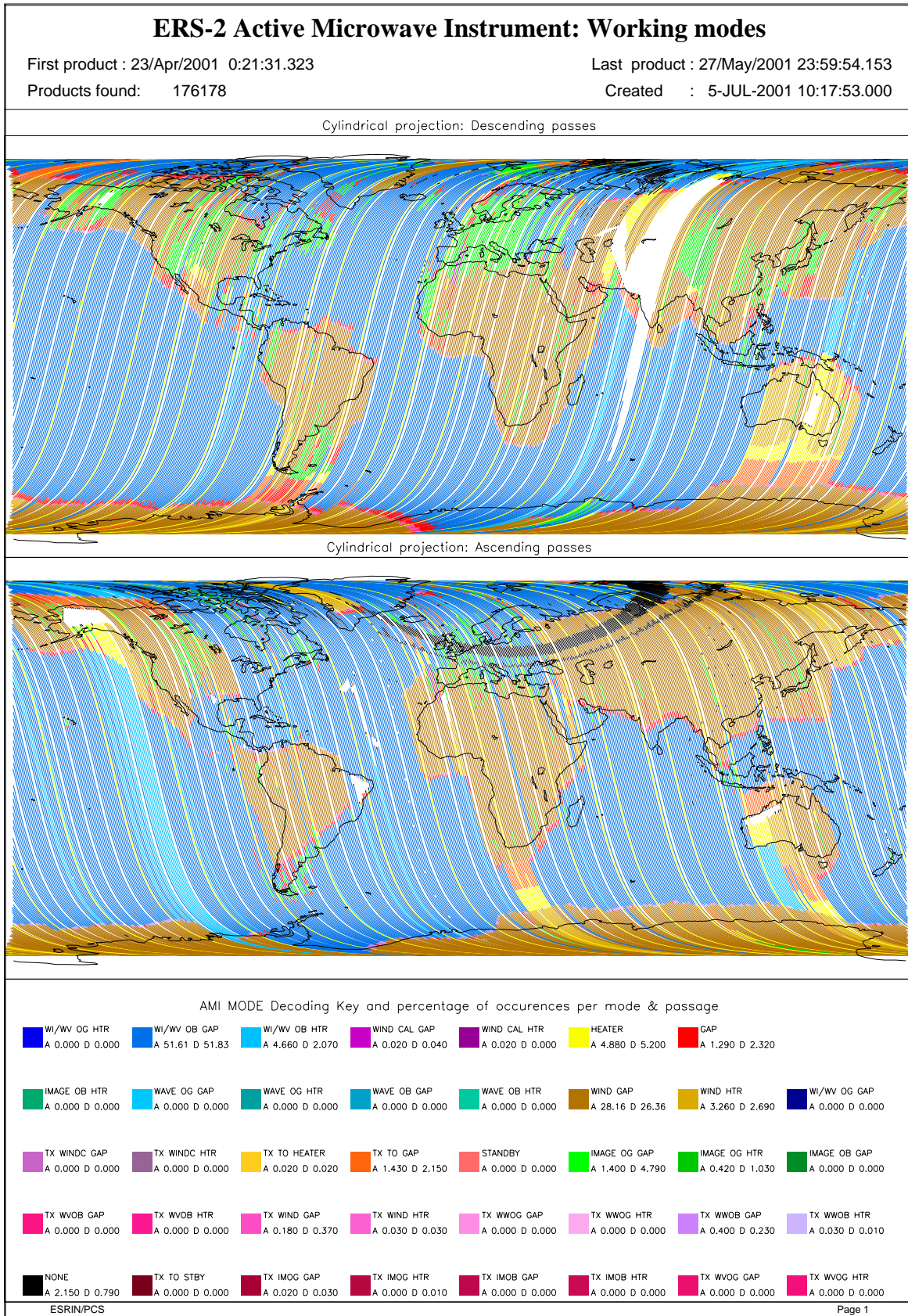


FIGURE 34. ERS-2 AMI activity during cycle 63.

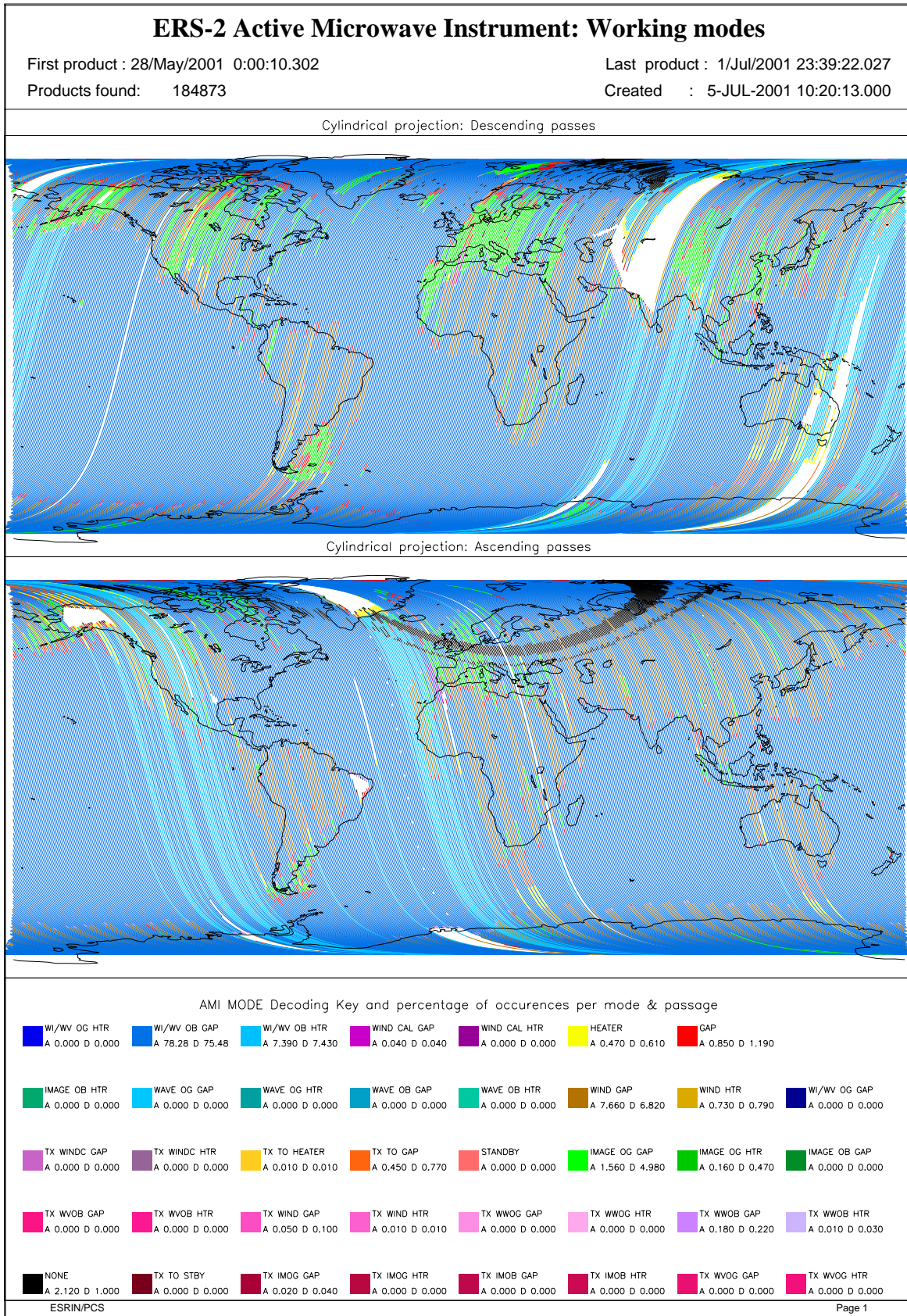


FIGURE 35. ERS-2 AMI activity during cycle 64.

The PCS carries out a quality control of the winds generated from the WSCATT data. The activity is split in two main areas: the first one includes a routine analysis of the fast Delivery Products disseminated to the users, the second one is focused on the improvement of the CMOD-4 (the operative ESA wind retrieval algorithm) for high wind speed (for more information see on the Web site <http://pcswww.esrin.esa.it> the Cyclone Tracking home page). External contributions to this quality control come also from ECMWF and UK-Met Office.

The routine analysis is summarized in the plots of figure 36; from top to bottom:

- the monitoring of the valid sigma-nought triplets per day.
- the evolution of the wind direction quality. The ERS wind direction (for all nodes and only for those nodes where the ambiguity removal has worked properly) is compared with the ECMWF forecast. The plot shows the percentage of nodes for which the difference falls in the range -90.0, +90.0 degrees.
- the monitoring of the percentage of nodes whose ambiguity removal works successfully.
- the comparison of the wind speed deviation: (bias and standard deviation) with the ECMWF forecast.

The results since August 6<sup>th</sup>, 1996 until EBM operations can be summarized (apart from the events given in Table 7) as:

- a stable number of valid sigma-nought acquired per day with a small increase after June 29<sup>th</sup>, 1999 due to the dissemination in fast delivery of the data acquired in the Prince Albert station.
- an accurate wind direction for roughly 93% of the nodes, a success in the ambiguity removal for more than 90.0% of the nodes.

The ERS-2 wind speed shows an absolute bias of roughly 0.5 m/s and a standard deviation that ranges from 2.5 m/s to 3.5 m/s with respect to the ECMWF forecast. The wind speed bias and its standard deviation have a seasonal pattern due to the different winds distribution between the winter and summer season.

It is important to note that only after the end of calibration phase (mid March 1996) the wind products have reached high quality.

Two important changes affect the speed bias plot: the first is on June 3<sup>rd</sup>, 1996 and it is due to the switch from ERS-1 to ERS-2 data assimilation in the meteorological model. The second change, which occurred at the beginning of September 1997, is due to the new monitoring and assimilation scheme in ECMWF algorithms (4D-Var).

Since 19<sup>th</sup> April 1999 two set of meteo-table (meteorological forecast centred at 00:00 and 12:00 of each day) are used in the ground processing. With this new strategy the data are processed using the 18 and 24 hours meteorological forecast instead of the 18, 24, 30 36 hours forecast. The data processed with the 18-24 hours tables instead of 30-36 hours tables have an increase in the number of ambiguity removed nodes but no important improvements are shown, on average, in the daily statistics.

Since 25<sup>th</sup> August 1999 a new LRDPF software (version 8500) is operative in the ground stations. With this upgrade the LRDPF is year 2000 compatible; no changes were introduced in the scatterometer data processing.

The mono-gyro AOCS configuration (see report for cycle 50) that was operative from 7<sup>th</sup> February 2000 to 17<sup>th</sup> January 2001 did not affect the wind data performance.

The new AOCS configuration (gyro-less EBM) had a very negative impact in the data quality.

The number of valid nodes has a clear drop from 190000 per day to 9000 per day. The overall Scatterometer transfer function is not matched with the received echo (Doppler shift in the received signal due to degraded satellite attitude) and this fact caused the decrease of the signal to noise ratio and as consequence many nodes are discarded by the wind retrieval algorithm. Moreover the sigma nought are not calibrated (the distance to the cone is high, in particular for the nodes at far range) and the wind speed bias is around 1.5 m/s.

During the ZGM commissioning phase only an improvements in the number of valid nodes has been noted. The improvement is mainly linked with the increase of the signal to noise ratio.

The number of valid nodes passed from 9000 per day (EBM) to 16000 per day during the ZGM commissioning. The wind speed bias stilt remains to the high value of 1.5 m/s.

Since 17<sup>th</sup> January 2001 no Scatterometer data are disseminated to the users. The actual ground processing is not able to assure calibrated data and the quality of the wind products is very poor.

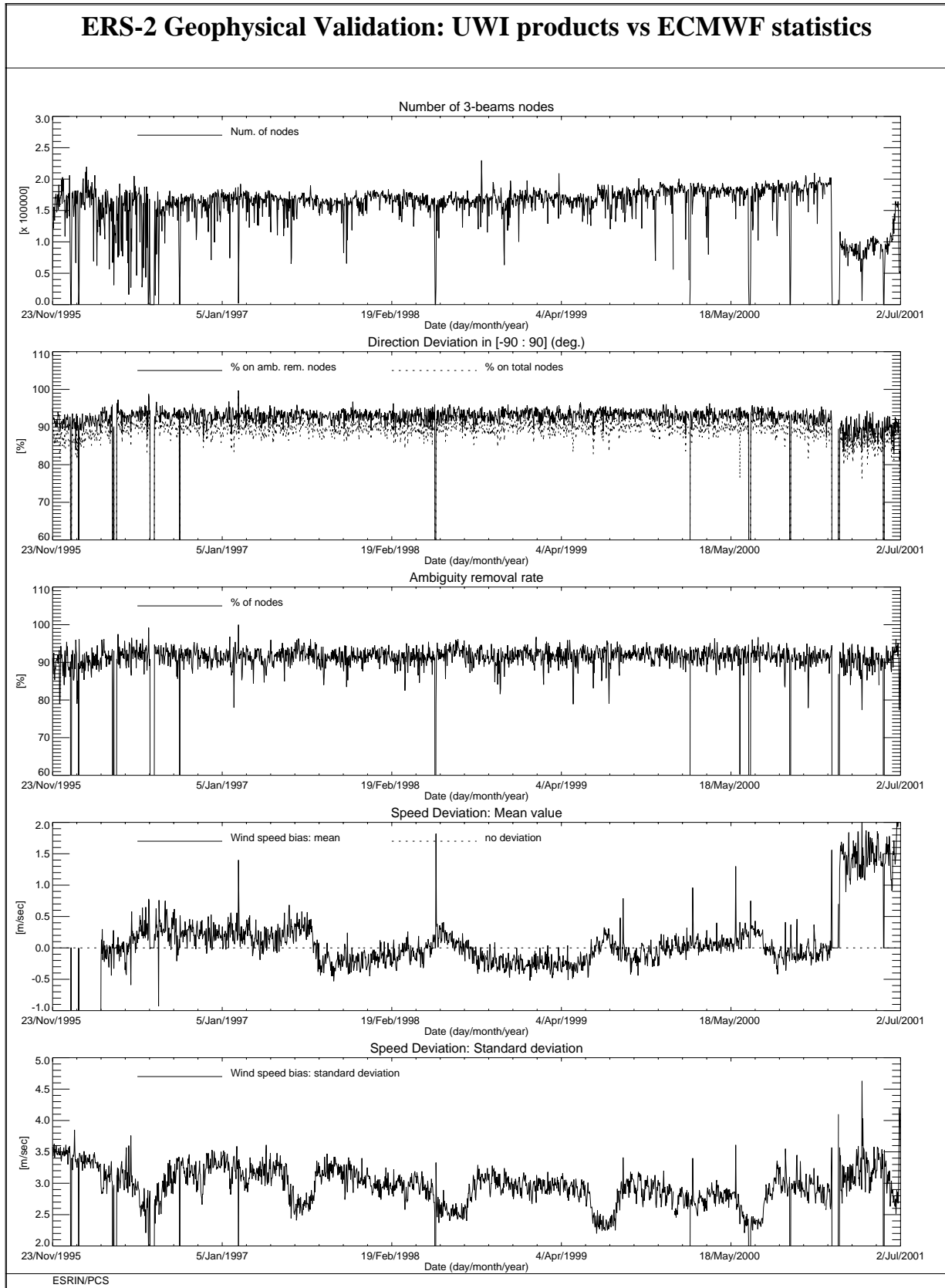


FIGURE 36. ERS-2 Scatterometer: wind products performance since the beginning of the mission.